

1 **ON THE ACTIVE FLUX SCHEME FOR HYPERBOLIC PDES WITH**  
2 **SOURCE TERMS\***

3 WASILIJ BARSUKOW<sup>†</sup>, JONAS P. BERBERICH<sup>‡</sup>, AND CHRISTIAN KLINGENBERG<sup>‡</sup>

4 **Abstract.** The active flux scheme is a finite volume scheme with additional point values dis-  
5 tributed along the cell boundary. It is third order accurate and does not require a Riemann solver:  
6 the initial value problem at the particular points is solved instead. The intercell flux is then obtained  
7 from the evolved values along the cell boundary by quadrature. This paper focuses on the conceptual  
8 extension of active flux to include source terms, and thus for simplicity assumes the homogeneous  
9 part of the equations linear. To a large part the treatment of the source terms is independent of the  
10 choice of the homogeneous part of the system. Additionally, only systems are considered which admit  
11 characteristics (instead of characteristic cones). This is the case for scalar equations in any number  
12 of spatial dimensions and systems in one spatial dimension. Here, we succeed to extend the active  
13 flux method to include (possibly nonlinear) source terms while maintaining third order accuracy of  
14 the method. This requires a novel (approximate) operator for the evolution of point values and a  
15 modified update procedure of the cell average. For linear acoustics with gravity, it is shown how to  
16 achieve a well-balanced / stationarity preserving numerical method.

17 **Key words.** finite volume methods, active flux, source terms, balance laws, well-balanced  
18 methods, gravity

19 **AMS subject classifications.** 35L65, 35L45, 65M08

20 **1. Introduction.** Numerous phenomena of the physical world are modeled by  
21 hyperbolic balance laws (conservation laws augmented by source terms). This includes  
22 gas dynamics, the motion of water waves, plasma physics and even general relativity.  
23 Often physical modeling requires to include source terms, and conservation is modified  
24 due to creation or annihilation of some of the evolved quantities. Chemical reactions,  
25 for example, change the number density of a species and produce or absorb heat (i.e.  
26 internal energy). Gravity accelerates matter downwards and creates momentum. In  
27 the shallow water model describing the motion of a free water surface the bottom  
28 topography enters the equations through a source term. Rewriting the hydrodynamic  
29 equations in a different coordinate system (e.g. in polar coordinates) makes geometric  
30 source terms appear. All these applications require reliable numerical methods which  
31 are able to deal with source terms.

32 Reliable numerical methods for hyperbolic conservation laws with source terms  
33 first need to perform well in the homogeneous case. This means for example that  
34 they need to cope with discontinuities / weak solutions and with phenomena arising  
35 in multiple spatial dimensions, such as involutions and non-trivial stationary states.  
36 This requirement has led [ER13, FR15] to suggest *active flux*, an extension of the finite  
37 volume method. Additionally to the cell average, this scheme evolves point values  
38 located at the cell boundary. The update of the point values is achieved by using  
39 an evolution operator that includes multi-dimensional information. The presence of  
40 the point values along the cell boundary then allows to compute the intercell flux

---

\*Submitted to the editors DATE.

**Funding:** WB was supported by the German Academic Exchange Service (DAAD) with funds from the German Federal Ministry of Education and Research (BMBF) and the European Union (FP7-PEOPLE-2013-COFUND – grant agreement no. 605728) as well as by the Deutsche Forschungsgemeinschaft (DFG) through project 429491391 (BA 6878/1-1).

<sup>†</sup>Institute of Mathematics, Zurich University, 8057 Zurich, Switzerland  
(wasilij.barsukow@math.uzh.ch).

<sup>‡</sup>Wuerzburg University, Emil-Fischer-Strasse 40, 97074 Wuerzburg, Germany.

41 via quadrature. It has been shown in [BHKR19] that this scheme is stationarity  
 42 preserving and vorticity preserving for linear acoustics without any fix. It is third  
 43 order accurate. Extensions to nonlinear systems have been recently suggested e.g. in  
 44 [Fan17, HKS19, Bar19a]. Active flux therefore seems to be promising for resolving  
 45 many of the structure preservation problems that currently available methods are  
 46 facing (an overview of existing methods for balance laws is given below).

47 In view of the many applications that involve source terms, this paper therefore  
 48 aims at deriving the necessary modifications for active flux to be applicable to balance  
 49 laws while retaining its third order accuracy. Including the source term requires a  
 50 number of modifications. The homogeneous part of the equations therefore is for  
 51 simplicity assumed to be a linear hyperbolic system for which characteristics are  
 52 available. This is the case for scalar equations in any number of spatial dimensions  
 53 and for systems in one spatial dimension. For multi-dimensional systems, the concept  
 54 of characteristics needs to be replaced by characteristics cones. In the homogeneous  
 55 case, active flux has been used for this situation as well ([ER13, BHKR19]), but an  
 56 extension to inhomogeneous systems in multi-d, and to nonlinear systems remains  
 57 subject of future work. To a large part, the strategies presented in this paper will,  
 58 however, remain valid when the homogeneous part of the equations is nonlinear as  
 59 well, and even for nonlinear multi-dimensional systems.

60 As soon as a source term is added to a hyperbolic system, new stationary states  
 61 arise which often are of particular interest. The stationarity is due to the flux di-  
 62 vergence being equal to the source term. Many areas of application of balance laws  
 63 involve studies of dynamics on top of such an equilibrium (e.g. astrophysics, meteorol-  
 64 ogy, tsunami modeling, ...). This requires the numerical method to be very accurate  
 65 on the stationary states in order to avoid spurious, artificial perturbations. Therefore  
 66 the error of a numerical solution representing one of those stationary states should  
 67 not increase with time, thus allowing the simulation to run for a long time.

68 Numerical methods which achieve this are called *well-balanced*, introduced in  
 69 [GL96]. They make sure that the discretization of the flux divergence and the dis-  
 70 cretization of the source term match, and that the numerical method keeps the de-  
 71 sired stationary state exactly stationary for any resolution of the grid. The concept  
 72 of well-balanced methods has been extensively used in the context of shallow water  
 73 equations with non-flat bottom topography (e.g. [ABB<sup>+</sup>04, BV94, LeV98] and refer-  
 74 ences therein). Here, the balance is the so-called lake-at-rest solution, which amounts  
 75 to an algebraic condition and can thus be given explicitly.

76 Another area in which well-balanced methods have high relevance is the simula-  
 77 tion of hydrodynamic processes using compressible Euler equations with gravitational  
 78 source term. The so-called hydrostatic state (stationary state with no velocity) is de-  
 79 scribed by one PDE for two unknown functions. There are many hydrostatic states,  
 80 depending on the additional thermodynamical relation that one chooses in order to  
 81 close this PDE. The fact that the stationary state is itself given by a differential  
 82 equation that cannot be integrated makes well-balancing much more delicate in this  
 83 context. There are two different ways which are currently used to construct well-  
 84 balanced methods for the Euler equations with gravity. The first and more traditional  
 85 way is to restrict the class of hydrostatic solutions which are balanced exactly or to  
 86 choose a particular, but arbitrary hydrostatic state (e.g. [CL94, LGB11, DZBK16,  
 87 CK15, BCK16, CCK<sup>+</sup>18, BCKR19, BCK19]). This is advantageous in all those ap-  
 88 plications where the stationary state is known, and the evolution of perturbations  
 89 around it shall be studied. If no information on the stationary state can be as-  
 90 sumed, then the only way to proceed is to make sure that the stationary states of the

91 numerical method are fulfilling some *discretization* of the corresponding PDE (e.g.  
 92 [DZBK14, KM16, BKCK20]).

93 For linear numerical methods a theory of such *stationarity preserving* methods  
 94 was given in [Bar19b], with a particular emphasis on this latter, more complicated,  
 95 situation of the stationary states given by PDEs, and not by algebraic relations. It  
 96 turns out that many standard numerical methods add diffusion even to those states  
 97 that should remain stationary. The set of states that are actually kept stationary by  
 98 such methods is very small (e.g. uniform constants). Stationarity preserving methods  
 99 do not apply diffusion to certain discrete data. These data are described by a discrete  
 100 version of the PDE governing the stationary states. Stationarity preserving methods  
 101 thus keep stationary a much larger set of initial data. Independently of how these  
 102 discrete equations actually look like, it is their existence that makes a qualitative  
 103 difference. In a non-stationarity-preserving method, initial data sampled from an  
 104 analytic stationary state will decay due to the diffusion and become unrecognizable  
 105 in the end. In a stationarity preserving method, these initial data will evolve towards  
 106 one of the many discrete stationary states approximating the steady PDE, and will  
 107 remain there forever (up to machine precision). The long-time numerical solution will  
 108 then indeed approximate the analytic stationary state. For more details, see [Bar19b].  
 109 In this paper we understand the concept of well-balancing in this sense of stationarity  
 110 preservation.

111 In this paper, after extending the active flux scheme to include source terms, we  
 112 construct a well-balanced active flux method for the equations of acoustics with grav-  
 113 ity. The hydrostatic solutions of acoustics with gravity are comparable to those of the  
 114 compressible Euler equations with gravity, since they are given via the same under-  
 115 determined differential equation. We show that the active flux scheme endowed with  
 116 an exact evolution operator is intrinsically well-balanced in this way. In practice, an  
 117 approximate evolution operator needs to be used. Hence we introduce a modification  
 118 of the approximate evolution operator which makes the scheme well-balanced even  
 119 upon usage of an approximate evolution operator.

120 The paper is organized as follows: After the active flux scheme for homogeneous  
 121 problems is introduced in section 2, the modifications necessary for including source  
 122 terms are discussed. Section 3 discusses the evolution operators necessary for the  
 123 update of the point values. Section 4 is devoted to the modifications in the update  
 124 of the average. Here, the focus lies on linear systems of equations with possibly  
 125 nonlinear source terms in one spatial dimension and on linear advection in multiple  
 126 spatial dimensions. Section 5 discusses well-balancing of active flux for linear acoustics  
 127 with gravity. Section 6 finally demonstrates numerically that the new method attains  
 128 third order accuracy with linear and nonlinear source terms, can be used to compute  
 129 Riemann problems, and displays well-balanced behavior for stationary states.

130 This work can be seen in the larger context of the quest for structure preserving  
 131 numerical methods, of which well-balanced methods form an example. Extending  
 132 these results to nonlinear hyperbolic equations with source terms and thus combining  
 133 the structure preserving properties of active flux remains subject of future work.  
 134 However, the procedures suggested in this paper are formulated with as little reference  
 135 to the linearity of the equations as possible.

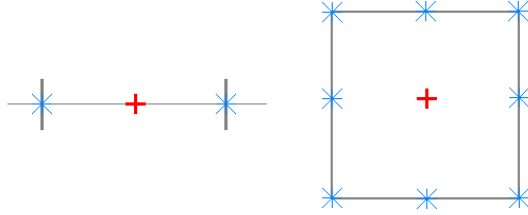


FIG. 1. The degrees of freedom used for active flux. Stars indicate the location of point values, and the cross (placed in the center symbolically) refers to the cell average. Left: One spatial dimension. Right: Two spatial dimensions.

136 **2. The active flux scheme.** Consider the initial value problem for an  $m \times m$   
 137 system of hyperbolic balance laws in  $d$  spatial dimensions<sup>1</sup>

$$138 \quad (2.1) \quad \partial_t q + \nabla \cdot \mathbf{f}(q) = s(q) \quad q : \mathbb{R}_0^+ \times \mathbb{R}^d \rightarrow \mathbb{R}^m, f, s : \mathbb{R}^m \rightarrow \mathbb{R}^m$$

$$139 \quad (2.2) \quad q(0, \mathbf{x}) := q_0(\mathbf{x})$$

141 This section reviews the general idea of the active flux scheme. Some of the details  
 142 then depend on the particular equation that is to be solved. After the general concept  
 143 is outlined, the details that make it applicable to hyperbolic balance laws are discussed  
 144 in sections 3 and 4.

145 **2.1. Degrees of freedom in the active flux scheme.** The active flux scheme  
 146 ([ER13, BHKR19], first introduced in [VL77]) is an extension of the finite volume  
 147 scheme. The active flux scheme evolves both the cell average and point values which  
 148 are distributed along the cell boundary. In particular, here the following two choices  
 149 are considered (see Figure 1):

- 150 • In one spatial dimension, there is a point value  $q_{i+\frac{1}{2}}$  located at each cell  
 151 interface  $x_{i+\frac{1}{2}}$ . Thus every cell has access to one cell average  $\bar{q}_i$  and two  
 152 point values at its interfaces.
- 153 • On Cartesian grids in two spatial dimensions, there is a point value  $q_{i+\frac{1}{2},j}$ ,  
 154  $q_{i,j+\frac{1}{2}}$  at each edge midpoint and one at each node  $q_{i+\frac{1}{2},j+\frac{1}{2}}$ . Every cell has  
 155 access to one cell average  $\bar{q}_{ij}$  and 8 point values distributed along the cell  
 156 interface.

157 Note that the point values at cell interfaces are shared by the adjacent cells. Thus,  
 158 in one spatial dimension, on average there are 2 degrees of freedom per cell: 1 cell  
 159 average and 2 interface values shared each by 2 cells. In two spatial dimensions  
 160 in the setup as described above there are 4 degrees of freedom per cell: 1 cell average, 4  
 161 edge values, each shared by two cells and 4 node values each shared by 4 cells.

162 Note also that active flux does not use a staggered grid. The degrees of freedom  
 163 at the cell boundaries are not averages over staggered volumes, but point values. This  
 164 also explains why there is no notion of a conservative update for these, because this  
 165 concept only applies to averages. The update of the cell average in the active flux  
 166 method is, of course, conservative (see below).

167 **2.2. Update of the cell average.** As the active flux scheme is an extension of  
 168 the finite volume scheme, given a numerical flux, the update of the average happens in

<sup>1</sup>In this paper, indices never denote derivatives. Boldface symbols denote vectors that have the same dimension as the space.

169 the same way as for finite volume schemes. In this section, this finite volume aspect of  
 170 active flux is described in an arbitrary number of spatial dimensions. The numerical  
 171 flux, however, is obtained very differently in the active flux scheme ([ER13, FR15]).  
 172 This is then described in detail in section 4.

173 Consider the computational domain to be subdivided into polygonal computa-  
 174 tional cells. Upon integration of (2.1) over one time step  $[t^n, t^n + \Delta t]$  and over  
 175 one computational cell  $\mathcal{C}$  one obtains an evolution equation for the cell average  
 176  $\bar{q}_{\mathcal{C}} := \frac{1}{|\mathcal{C}|} \int_{\mathcal{C}} d\mathbf{x} q(t, \mathbf{x})$ :

$$177 \quad \frac{\bar{q}_{\mathcal{C}}^{n+1} - \bar{q}_{\mathcal{C}}^n}{\Delta t} + \frac{1}{|\mathcal{C}|} \frac{1}{\Delta t} \int_{t^n}^{t^n + \Delta t} dt \int_{\partial\mathcal{C}} d\sigma \mathbf{n} \cdot \mathbf{f}(q(t, \mathbf{x})) =$$

$$178 \quad \frac{1}{\Delta t} \int_{t^n}^{t^n + \Delta t} dt \frac{1}{|\mathcal{C}|} \int_{\mathcal{C}} d\mathbf{x} s(q(t, \mathbf{x}))$$

179

180 Here, as usual, the index of the time step is denoted as a superscript and  $q_{\mathcal{C}}^n$  denotes  
 181 the average in cell  $\mathcal{C}$  at time  $t^n$ . The boundary  $\partial\mathcal{C}$  consists of edges  $e$ , such that one  
 182 can rewrite

$$183 \quad \frac{\bar{q}_{\mathcal{C}}^{n+1} - \bar{q}_{\mathcal{C}}^n}{\Delta t} + \frac{1}{|\mathcal{C}|} \frac{1}{\Delta t} \int_{t^n}^{t^n + \Delta t} dt \sum_{e \in \partial\mathcal{C}} \int_e d\sigma \mathbf{n}_e \cdot \mathbf{f}(q(t, \mathbf{x})) =$$

$$184 \quad \frac{1}{\Delta t} \int_{t^n}^{t^n + \Delta t} dt \frac{1}{|\mathcal{C}|} \int_{\mathcal{C}} d\mathbf{x} s(q(t, \mathbf{x}))$$

185

186 The vector  $\mathbf{n}_e$  is the outward unit normal of edge  $e$ . This expression, so far exact,  
 187 becomes a finite volume scheme upon replacing the exact normal flux and source  
 188 averages by suitable approximations  $\hat{f}_e$  and  $\hat{s}_{\mathcal{C}}$ :

$$189 \quad (2.3) \quad \frac{\bar{q}_{\mathcal{C}}^{n+1} - \bar{q}_{\mathcal{C}}^n}{\Delta t} + \frac{1}{|\mathcal{C}|} \sum_{e \in \partial\mathcal{C}} |e| \hat{f}_e = \hat{s}_{\mathcal{C}}$$

190

191 with

$$192 \quad (2.4) \quad \hat{f}_e \simeq \frac{1}{\Delta t} \int_{t^n}^{t^n + \Delta t} dt \frac{1}{|e|} \int_e d\sigma \mathbf{n}_e \cdot \mathbf{f}(q(t, \mathbf{x}))$$

$$193 \quad (2.5) \quad \hat{s}_{\mathcal{C}} \simeq \frac{1}{\Delta t} \int_{t^n}^{t^n + \Delta t} dt \frac{1}{|\mathcal{C}|} \int_{\mathcal{C}} d\mathbf{x} s(q(t, \mathbf{x}))$$

194

195 Usual finite volume schemes introduce a (piecewise continuous) reconstruction  
 196 of the averages, and obtain the numerical flux by an exact or approximate short-  
 197 time evolution of this reconstruction. For example, introducing a piecewise constant  
 198 function whose averages match the given cell averages, and solving the Riemann  
 199 problems at the cell interfaces allows to compute a numerical flux.

200 The active flux scheme does not need this. Indeed, the point values along the  
 201 boundary can be used to immediately approximate (2.4)–(2.5) by quadrature. The

202 desired properties (most importantly the desired order of accuracy) of the resulting  
 203 scheme dictate the number of point values along each edge and also the points in time  
 204 at which these point values need to be available.

205 The source term also contributes to the update of the cell average. The quadrature  
 206 necessary to approximate the source term average (2.5) to sufficient order in space  
 207 and time is suggested in this paper for the first time and discussed in section 4.

208 **2.3. Update of the point values.** The cell average update, and in particular  
 209 the computation of the intercell fluxes, requires accurate point values at the cell  
 210 boundary to be available.

211 First consider the case where the source term vanishes:  $s = 0$ . For third order of  
 212 accuracy, the integrals in (2.4) need to be approximated by Simpson's rule. For the  
 213 integration in space this can easily be achieved using the available point values at each  
 214 cell interface as described in section 2.1. For the integration in time all point values  
 215 need to be available at  $t^n, t^n + \frac{\Delta t}{2}$  and  $t^n + \Delta t$ . Altogether this yields a space-time  
 216 Simpson rule.

217 In order to obtain sufficiently accurate time evolved point values, in [VL77] it has  
 218 been suggested to reconstruct the data and to use an exact evolution operator. An  
 219 exact evolution operator generally is unavailable for nonlinear problems, and there-  
 220 fore in [Fan17, HKS19, Bar19a] approximate evolution operators have been proposed.  
 221 Even for linear systems of hyperbolic balance laws it is generally very difficult to ob-  
 222 tain closed-form exact evolution operators, as is shown in section 3.2. Therefore the  
 223 point values in the active flux scheme shall be evolved using a sufficiently high order  
 224 *approximate* evolution operator applied to a reconstruction of the discrete data. An  
 225 exact evolution operator provides the necessary upwinding in order to guarantee sta-  
 226 bility, and an approximate evolution operator needs to do the same. The approximate  
 227 evolution operator is introduced in section 3.3.

228 **2.4. Reconstruction.** The reconstruction shall interpolate the point values and  
 229 its average over the computational cell shall match the given cell average. In the  
 230 following, to simplify notation, in one spatial dimension a uniform grid is assumed,  
 231 although the reconstruction can immediately be generalized to nonuniform grids. In  
 232 two spatial dimensions, a Cartesian grid is used. As mentioned in section 2.1, in  
 233 one spatial dimension every cell has access to 3 degrees of freedom which makes a  
 234 parabolic reconstruction natural. With the above-mentioned setup it is unique and  
 235 reads ([VL77, FR15])

$$236 \quad (2.6) \quad q_{\text{recon},i}(x) = -3(2\bar{q}_i - q_{i-\frac{1}{2}} - q_{i+\frac{1}{2}}) \frac{(x - x_i)^2}{\Delta x^2}$$

$$237 \quad (2.7) \quad + (q_{i+\frac{1}{2}} - q_{i-\frac{1}{2}}) \frac{x - x_i}{\Delta x} + \frac{6\bar{q}_i - q_{i-\frac{1}{2}} - q_{i+\frac{1}{2}}}{4} \quad x \in [x_{i-\frac{1}{2}}, x_{i+\frac{1}{2}}]$$

239 In two spatial dimensions as described above, every cell has access to 9 degrees of  
 240 freedom, and there is a unique biparabolic reconstruction, which reads

$$\begin{aligned}
 q_{\text{recon},ij}(\xi\Delta x, \eta\Delta y) &:= \frac{9}{4}\bar{q}_{ij}(-1+4\xi^2)(-1+4\eta^2) \\
 &\quad - \frac{1}{4}q_{\text{W}}(-1-4\xi+12\xi^2)(-1+4\eta^2) \\
 &\quad - \frac{1}{4}q_{\text{E}}(-1+4\xi+12\xi^2)(-1+4\eta^2) \\
 &\quad - \frac{1}{4}q_{\text{S}}(-1+4\xi^2)(-1-4\eta+12\eta^2) \\
 241 \quad (2.8) \quad &\quad - \frac{1}{4}q_{\text{N}}(-1+4\xi^2)(-1+4\eta+12\eta^2) \\
 &\quad + \frac{1}{16}q_{\text{SW}}(-1+2\xi)(-1+2\eta)(-1-2\eta+2\xi(-1+6\eta)) \\
 &\quad + \frac{1}{16}q_{\text{SE}}(1+2\xi)(-1+2\eta)(1+2\eta+2\xi(-1+6\eta)) \\
 &\quad + \frac{1}{16}q_{\text{NW}}(-1+2\xi)(1+2\eta)(1-2\eta+2\xi(1+6\eta)) \\
 &\quad + \frac{1}{16}q_{\text{NE}}(1+2\xi)(1+2\eta)(-1+2\eta+2\xi(1+6\eta))
 \end{aligned}$$

242

243 with  $\xi := x/\Delta x$ ,  $\eta := y/\Delta y$  and

$$244 \quad (2.9) \quad q_{\text{NE}} = q_{i+\frac{1}{2},j+\frac{1}{2}} \quad q_{\text{NW}} = q_{i-\frac{1}{2},j+\frac{1}{2}} \quad q_{\text{SW}} = q_{i-\frac{1}{2},j-\frac{1}{2}} \quad q_{\text{SE}} = q_{i+\frac{1}{2},j-\frac{1}{2}}$$

$$245 \quad (2.10) \quad q_{\text{N}} = q_{i,j+\frac{1}{2}} \quad q_{\text{S}} = q_{i,j-\frac{1}{2}} \quad q_{\text{E}} = q_{i+\frac{1}{2},j} \quad q_{\text{W}} = q_{i-\frac{1}{2},j}$$

247 Note that both reconstructions are globally continuous, but generally not contin-  
 248 uously differentiable at the cell interfaces.

249 **2.5. Overview of the algorithm.** The overall algorithm of active flux is as  
 250 follows:

- 251 1. Given cell averages and point values, compute a reconstruction according to  
 252 section 2.4.
- 253 2. Use the reconstruction as initial data in the update of the point values. The  
 254 choices of evolution operators considered so far are discussed in section 2.3  
 255 and evolution operators in presence of source terms are suggested in section  
 256 3.3 below.
- 257 3. Given the updated point values along the cell interfaces, compute the inter-  
 258 cell fluxes via quadrature (sections 2.2 and 4 for the homogeneous and the  
 259 inhomogeneous cases, respectively).
- 260 4. Update the cell averages via (2.3).

261 A CFL-type condition arises in the update of the point values: the domain of  
 262 dependence of the evolution operator needs to be contained in the neighbouring cells.  
 263 Denoting by  $\lambda_{\text{max}}$  the maximum speed of propagation, the time step needs to be  
 264 chosen as

$$265 \quad (2.11) \quad \Delta t \leq \frac{L_{\text{min}}}{\lambda_{\text{max}}}$$

266

267 where  $L_{\text{min}} = \Delta x$  in one spatial dimension, and  $L_{\text{min}} = \frac{1}{2} \min(\Delta x, \Delta y)$  in two spatial  
 268 dimensions, when the point values are distributed as described in section 2.1.

269 **3. Evolution of the point values in presence of a source term.** The  
 270 evolution of the point values needs to account for the source term. Additionally, in  
 271 this paper a special focus shall lie on structure preservation properties of the resulting  
 272 scheme. In the homogeneous case such properties have been observed upon usage of  
 273 an exact evolution operator ([BHKR19]). In presence of a source term, one needs to  
 274 use an approximate evolution operator (section 3.3), but should nevertheless aim at  
 275 making it such that it does not spoil structure preservation (see section 5).

276 For certain equations, the inhomogeneous problem admits an exact solution (sec-  
 277 tions 3.1–3.2). This is valuable in order to assess specific properties of the numerical  
 278 method later.

279 **3.1. Linear advection with a source term in multiple spatial dimen-**  
 280 **sions.** Consider a scalar equation ( $m = 1$ ) and  $\mathbf{f}(q) = \mathbf{U}q$  with  $\mathbf{U} \in \mathbb{R}^d$ . Then

$$281 \quad (3.1) \quad \partial_t q + \mathbf{U} \cdot \nabla q = s(q)$$

283 amounts to the ODE

$$284 \quad (3.2) \quad \frac{d}{dt} q = s(q)$$

286 along the straight characteristic of velocity  $\mathbf{U}$ . This ODE can be easily solved ana-  
 287 lytically:

$$288 \quad (3.3) \quad \int_{q_0(\mathbf{x}-\mathbf{U}t)}^{q(t,\mathbf{x})} \frac{dp}{s(p)} = t$$

290 E.g. for  $s(q) = \kappa q$  this yields  $\ln \frac{q(t,\mathbf{x})}{q_0(\mathbf{x}-\mathbf{U}t)} = \kappa t$ , or

$$291 \quad (3.4) \quad q(t, \mathbf{x}) = q_0(\mathbf{x} - \mathbf{U}t) \exp(\kappa t)$$

293 and for  $s(q) = \kappa q^B$ ,  $B \neq 1$

$$294 \quad (3.5) \quad q(t, \mathbf{x}) = \left( (q_0(\mathbf{x} - \mathbf{U}t))^{1-B} + (1-B)\kappa t \right)^{\frac{1}{1-B}}$$

296 **3.2. Linear acoustics with gravity in one spatial dimension.** This section  
 297 has threefold purpose. First, it introduces the acoustic equations with a gravity  
 298 source term, which form a very useful system for the study of structure preservation  
 299 of numerical methods. This is the set of equations for which a well-balanced method  
 300 is derived in 5. This section also demonstrates the difficulties of finding an exact  
 301 solution to an inhomogeneous system even if it is linear. Finally, the exact solution  
 302 derived here is used later in order to assess the accuracy of the numerical method.

303 The equations of linear acoustics in one spatial dimension endowed with a gravity  
 304 source term read:

$$305 \quad (3.6) \quad \partial_t \rho + \partial_x v = 0$$

$$306 \quad (3.7) \quad \partial_t v + \partial_x p = \rho g \quad g \in \mathbb{R}$$

$$307 \quad (3.8) \quad \partial_t p + c^2 \partial_x v = 0$$

309 The corresponding homogeneous problem (linear acoustics) is the linearization of  
 310 the Euler equations around the background state of constant density  $\rho_{\text{bg}} = 1$ , constant



311 pressure  $p_{\text{bg}}$  and vanishing velocity. Then the speed of sound  $c = \sqrt{\frac{\gamma p_{\text{bg}}}{\rho_{\text{bg}}}}$  is a constant  
 312 ( $\mathbb{R} \ni \gamma > 1$ ). The full system (3.6)–(3.8) can be understood as a particular kind of a  
 313 linearization of the Euler equations with gravity<sup>2</sup>

$$314 \quad (3.9) \quad \partial_t \rho + \partial_x(\rho v) = 0$$

$$315 \quad (3.10) \quad \partial_t(\rho v) + \partial_x(\rho v^2 + p) = \rho g$$

$$316 \quad (3.11) \quad \partial_t e + \partial_x(v(e + p)) = 0$$

$$317 \quad (3.12) \quad e = \frac{p}{\gamma - 1} + \frac{1}{2}\rho v^2 - \rho g x$$

319 The static (stationary and  $v = 0$ ) states of (3.9)–(3.11) are governed by  $\partial_x p = \rho g$ .  
 320 This equation can only be solved if e.g.  $\rho$  is given as a function of  $x$ , or if another  
 321 relation is provided between any two of the variables  $p, \rho, e$ . This multitude of possible  
 322 stationary states is reflected in the linearization (3.6)–(3.8). (This is the reason for  
 323 this particular choice of a linearization.) Observe that stationary states of (3.6)–  
 324 (3.8) also are governed by  $\partial_x p = \rho g$  and that  $p$  can only be computed if  $\rho$  is given  
 325 as a function of  $x$ , or if an additional relation is provided that links  $\rho$  and  $p$ . This  
 326 is an example of a so-called non-trivial stationary state as introduced in [Bar19b].  
 327 Examples of stationarity preserving schemes for (3.6)–(3.8) have been discussed in  
 328 [Bar18].

329 The exact solution of (3.6)–(3.8) is studied in the Appendix A. This solution is  
 330 not part of the suggested method but only serves auxiliary purposes, such as accuracy  
 331 checks. However it illustrates the difficulties encountered when solving linear systems  
 332 with sources. To the authors’ knowledge the exact solution to (3.6)–(3.8) is not  
 333 available in the literature so far.

334 **3.3. Runge-Kutta method for linear systems with a source.** Consider an  
 335  $m \times m$  linear system in characteristic variables:

$$336 \quad (3.13) \quad (\partial_t + \lambda_\ell \partial_x) Q_\ell = S_\ell(Q_1, \dots, Q_m) \quad \ell = 1, \dots, m$$

338 From now on, the capital letter  $Q$  denotes the characteristic variables of this particular  
 339 system, whereas  $q$  continues to denote a generic variable.

340 Recall the following theorem from [Bar19a]:

341 **THEOREM 3.1.** *Assume a hyperbolic CFL condition  $\Delta x / \Delta t \rightarrow \text{const}$  as  $\Delta t \rightarrow 0$ .  
 342 If the approximate evolution  $Q^{\text{approx}}(t, x)$  approximates the exact solution  $Q(t, x)$  for  
 343 fixed  $x$  at least as*

$$344 \quad (3.14) \quad Q^{\text{approx}}(t, x) = Q(t, x) + \mathcal{O}(t^3)$$

346 *and the quadrature rules used to approximate (2.4)–(2.5) yield the exact value up to  
 347 an error of  $\mathcal{O}(\Delta t^\alpha \Delta x^\beta)$ ,  $\alpha + \beta \geq 3$  then active flux formally achieves third order  
 348 accuracy.*

349 Note that the simple approach of evolving each component of the source term  
 350 along its associated characteristic

$$351 \quad (3.15) \quad Q_\ell(t, x) \simeq Q_{\ell,0}(x - \lambda_\ell t) + t S_\ell(Q_{1,0}(x - \lambda_\ell t), \dots, Q_{m,0}(x - \lambda_\ell t)) \quad \ell = 1, \dots, m$$

<sup>2</sup>Note that often the energy equation is written with a source term  $\rho g v$  appearing. This source term is unnecessary, as it can be removed by redefining the notion of total energy. When the total energy includes the potential energy  $-\rho g x$  due to gravity, the conservation form of the energy equation is restored. The source term in the momentum equation remains.

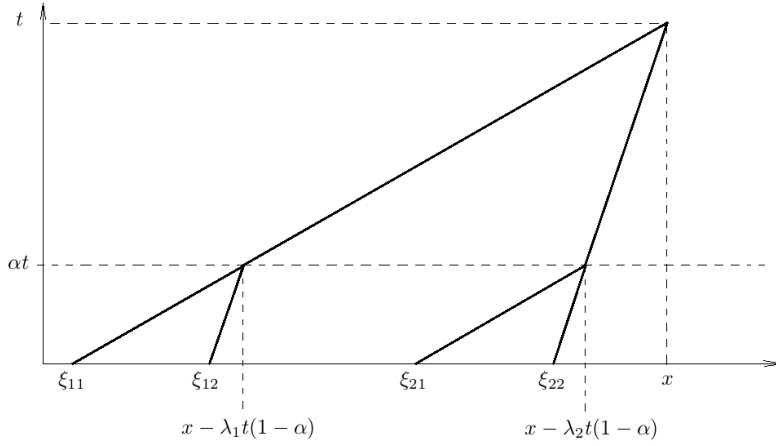


FIG. 2. Illustration of the intermediate solutions and the involved characteristics for the first step in the Runge-Kutta scheme.

353 fails to be accurate enough (the error is  $\mathcal{O}(t^2)$  instead of  $\mathcal{O}(t^3)$ ).

354 Recall the second order Runge-Kutta method for the ordinary differential equation

355 (3.16)  $\dot{q}(t) = s(t, q(t))$   $q : \mathbb{R}_0^+ \rightarrow \mathbb{R}$

357

358 (3.17)  $q^{(1)}(\alpha t) = q(0) + \alpha t s(0, q(0))$

359 (3.18)  $q(t) = q(0) + t \left(1 - \frac{1}{2\alpha}\right) s(0, q(0)) + t \frac{1}{2\alpha} s(\alpha t, q^{(1)}(\alpha t)) + \mathcal{O}(t^3)$

360

361 for any  $\alpha \in (0, 1)$ . In particular choosing  $\alpha = \frac{1}{2}$  (midpoint method) involves a  
 362 predictor value at half time step. This can be taken as inspiration for constructing a  
 363 sufficiently accurate approximate evolution operator:

364 THEOREM 3.2 (RK2 evolution operator). Choose (see Figure 2)

365 (3.19)  $\xi_{\ell k} := x - \lambda_{\ell} t(1 - \alpha) - \lambda_k \alpha t$

366 (3.20)  $Q_{k\ell}^* := Q_{k,0}(\xi_{\ell k}) + \alpha t S_k(Q_{1,0}(\xi_{\ell k}), \dots, Q_{m,0}(\xi_{\ell k}))$   $k, \ell = 1, \dots, m$

368 and

(3.21)

369  $Q_{\ell}^{(1)}(t, x) := Q_{\ell,0}(x - \lambda_{\ell} t) + \left(1 - \frac{1}{2\alpha}\right) S_{\ell}(Q_{1,0}(x - \lambda_{\ell} t), \dots, Q_{m,0}(x - \lambda_{\ell} t))t$

370 (3.22)  $+ \frac{t}{2\alpha} S_{\ell}(Q_{1\ell}^*, \dots, Q_{m\ell}^*)$   $\ell = 1, \dots, m$

371

372 Then, for all  $\alpha \in (0, 1)$

373 (3.23)  $Q_{\ell}^{(1)}(t, x) = Q_{\ell}(t, x) + \mathcal{O}(t^3)$   $\ell = 1, \dots, m$

374

375 Note that  $Q_{\ell j}^*$  approximates  $Q_{\ell}(\alpha t, x - \lambda_j t(1 - \alpha))$ .

376 *Proof.* By explicitly computing the first three terms of the Taylor series in  $t$  one  
 377 confirms the statement. The exact solution is

$$378 \quad (3.24) \quad Q_\ell(t, x) = Q_{\ell,0}(x) + t\partial_t Q_\ell \Big|_{t=0} + \frac{t^2}{2}\partial_t^2 Q_\ell \Big|_{t=0} + \mathcal{O}(t^3)$$

$$379 \quad (3.25) \quad = Q_{\ell,0}(x) + t(S_{\ell,0} - \lambda_\ell \partial_x Q_{\ell,0})$$

$$380 \quad (3.26) \quad + \frac{t^2}{2} \left( \sum_k \frac{\partial S_\ell}{\partial Q_k} (S_{k,0} - (\lambda_k + \lambda_\ell) \partial_x Q_{k,0}) + \lambda_\ell^2 \partial_x^2 Q_{\ell,0} \right) + \mathcal{O}(t^3)$$

381

382 where  $S_{\ell,0}$  denotes

$$383 \quad (3.27) \quad S_{\ell,0} := S_\ell(Q_{1,0}(x), \dots, Q_{m,0}(x))$$

385 and  $\frac{\partial S_\ell}{\partial Q_k}$  also is evaluated at  $x$ . Note that it has been used that  $\partial_x \lambda_\ell = 0$  (i.e. that the  
 386 homogeneous system is linear), but the source  $S$  can be any differentiable function of  
 387  $Q$ .

388 Expand now (3.22) ( $\ell = 1, \dots, m$ ):

$$389 \quad (3.28) \quad \partial_t Q_{k\ell}^* \Big|_{t=0} = -(\lambda_\ell(1 - \alpha) + \lambda_k \alpha) \partial_x Q_{k,0} + \alpha S_{k,0}$$

$$390 \quad (3.29) \quad \partial_t Q_\ell^{(1)}(t, x) = -\lambda_\ell \partial_x Q_{\ell,0}(x - \lambda_\ell t)$$

$$391 \quad (3.30) \quad + \left(1 - \frac{1}{2\alpha}\right) \left( t \sum_k \frac{\partial S_\ell}{\partial Q_k} \partial_x Q_{k,0}(x - \lambda_\ell t) (-\lambda_\ell) \right)$$

$$392 \quad (3.31) \quad + S_\ell(Q_{1,0}(x - \lambda_\ell t), \dots, Q_{m,0}(x - \lambda_\ell t))$$

$$393 \quad (3.32) \quad + \frac{1}{2\alpha} \left( t \sum_k \frac{\partial S_\ell}{\partial Q_k} \partial_t Q_{k\ell}^* + S_\ell(Q_{1\ell}^*, \dots, Q_{m\ell}^*) \right)$$

$$394 \quad (3.33) \quad \stackrel{t=0}{=} -\lambda_\ell \partial_x Q_{\ell,0} + S_{\ell,0}$$

$$395 \quad (3.34) \quad \partial_t^2 Q_\ell^{(1)}(t, x) \Big|_{t=0} = \lambda_\ell^2 \partial_x^2 Q_{\ell,0} + \left(1 - \frac{1}{2\alpha}\right) \left( 2 \sum_k \frac{\partial S_\ell}{\partial Q_k} \partial_x Q_{k,0} (-\lambda_\ell) \right)$$

$$396 \quad (3.35) \quad + \frac{1}{2\alpha} \left( 2 \sum_k \frac{\partial S_\ell}{\partial Q_k} \partial_t Q_{k\ell}^* \Big|_{t=0} \right)$$

$$397 \quad (3.36) \quad = \lambda_\ell^2 \partial_x^2 Q_{\ell,0} - \sum_k \frac{\partial S_\ell}{\partial Q_k} \left( \partial_x Q_{k,0} (\lambda_\ell + \lambda_k) - S_{k,0} \right) \quad \square$$

398

399 Obviously the two Taylor series agree up to terms  $\mathcal{O}(t^3)$ , which proves the statement.

400 **COROLLARY 3.3** (Midpoint method). *If  $\alpha = \frac{1}{2}$ , then for  $\ell, k = 1, \dots, m$*

$$401 \quad (3.37) \quad \xi_{\ell,j} := x - (\lambda_\ell + \lambda_j) \frac{t}{2}$$

$$402 \quad (3.38) \quad Q_{k\ell}^* := Q_{k,0}(\xi_{k\ell}) + \frac{t}{2} S_k(Q_{1,0}(\xi_{k\ell}), \dots, Q_{m,0}(\xi_{k\ell}))$$

$$403 \quad (3.39) \quad Q_\ell^{(1)}(t, x) := Q_{\ell,0}(x - \lambda_\ell t) + t S_\ell(Q_{1\ell}^*, \dots, Q_{m\ell}^*)$$

404

405 COROLLARY 3.4 (RK2 evolution operator for a scalar equation). *For a scalar*  
 406 *equation*

$$407 \quad (3.40) \quad (\partial_t + \lambda \partial_x)Q = S(Q)$$

409 *the algorithm reads*

$$410 \quad (3.41) \quad \xi := x - \lambda t$$

412 *and*

$$413 \quad (3.42) \quad Q^{(1)}(t, x) := Q_0(x - \lambda t) + \left(1 - \frac{1}{2\alpha}\right) S(Q_0(x - \lambda t))t$$

$$414 \quad (3.43) \quad + \frac{t}{2\alpha} S\left(Q_0(\xi) + \alpha t S(Q_0(\xi))\right)$$

416 For the equations (3.6)–(3.8) of linear acoustics with gravity,  $\lambda_1 = c = -\lambda_2$ ,  $\lambda_3 =$   
 417 0. The characteristic variables are

$$418 \quad (3.44) \quad Q_1 = \frac{p + cv}{2} \quad Q_2 = \frac{p - cv}{2} \quad Q_3 = -\frac{p}{c^2} + \rho$$

420 and the gravity source term then is

$$421 \quad (3.45) \quad S_1 = -S_2 = \frac{g}{2c}(Q_1 + Q_2) + \frac{cg}{2}Q_3 \quad S_3 = 0$$

423 **4. Update of the cell average in presence of a source term.** The update of  
 424 the cell average needs to include the space-time average of the source term according  
 425 to (2.3) of section 2.2. This space-time average needs to be approximated by a suitable  
 426 quadrature / approximation with sufficient order of accuracy. Active flux has a strong  
 427 focus on providing discrete degrees of freedom along the boundary which allow to  
 428 perform a quadrature along the boundary. However, the evaluation of the source  
 429 term for the update of the cell average involves an averaging over the cell volume. It  
 430 is more difficult to achieve the desired order of accuracy here, as the setup lacks the  
 431 quadrature points that would have been natural for this task. A quadrature formula  
 432 adapted to the geometry of the active flux method is derived here.

433 Active flux for equations with a source term is considered in [NR16] for stationary  
 434 problems, and for parabolic problems with slowly varying boundary conditions. In  
 435 these cases there is no need to use high order quadrature in time. Therefore the  
 436 method suggested there cannot be used here.

437 **4.1. One spatial dimension.** The numerical discretization (2.5)

$$438 \quad (4.1) \quad \hat{s}_C \simeq \frac{1}{\Delta t} \int_{t^n}^{t^n + \Delta t} dt \frac{1}{|C|} \int_C dx s(q(t, \mathbf{x}))$$

440 of the source term in (2.3) requires a space-time quadrature that is exact for parabolic  
 441 functions. The natural candidate would be Simpson's rule in both space and time (as  
 442 used for the numerical flux), but there are not enough quadrature points for it. For  
 443 example in one spatial dimension, the available information is

$t^{n+1}$	$q_{i-\frac{1}{2}}^{n+1}$	$q_{i+\frac{1}{2}}^{n+1}$
$t^{n+\frac{1}{2}}$	$q_{i-\frac{1}{2}}^{n+\frac{1}{2}}$	$q_{i+\frac{1}{2}}^{n+\frac{1}{2}}$
$t^n$	$q_{i-\frac{1}{2}}^{n+1}$	$q_{i+\frac{1}{2}}^n$
	$x_{i-\frac{1}{2}}$	$x_{i+\frac{1}{2}}$

444  
445 These are only 7 values (the box emphasizes that one of the values is a cell average,  
446 whereas the others are point values).

447 **4.1.1. Linear source term.** Consider first a linear source term, i.e.  $s'' = 0$ .  
448 Such source terms are relevant in practice (e.g. compressible Euler equations with  
449 gravity), and therefore it is worth dealing with them specifically as they allow for a  
450 simpler approach. For linear source it is possible to first find a quadrature for  $q$  and  
451 to apply  $s$  to the result. In order to find a quadrature formula for  $q$ , one needs to  
452 find a space-time polynomial  $p(t, x)$  of at least second degree which interpolates the  
453 available 7 data. Integrating this polynomial would yield a quadrature formula for  $q$ .  
454 Here we suggest to use

455 (4.2) 
$$\mathcal{P}(t, x) = (a_0 + a_1x + a_2t + a_3x^2 + a_4xt + a_5t^2) + a_6xt^2$$

457 There is a unique set of coefficients  $a_0, \dots, a_6$  which makes polynomial (4.2) fulfill

458 (4.3) 
$$\mathcal{P}(t^{n+1}, x_{i-\frac{1}{2}}) = q_{i-\frac{1}{2}}^{n+1} \qquad \mathcal{P}(t^{n+1}, x_{i+\frac{1}{2}}) = q_{i+\frac{1}{2}}^{n+1}$$

459 (4.4) 
$$\mathcal{P}(t^{n+\frac{1}{2}}, x_{i-\frac{1}{2}}) = q_{i-\frac{1}{2}}^{n+\frac{1}{2}} \qquad \mathcal{P}(t^{n+\frac{1}{2}}, x_{i+\frac{1}{2}}) = q_{i+\frac{1}{2}}^{n+\frac{1}{2}}$$

460 (4.5) 
$$\mathcal{P}(t^n, x_{i-\frac{1}{2}}) = q_{i-\frac{1}{2}}^n \qquad \int_{x_{i-\frac{1}{2}}}^{x_{i+\frac{1}{2}}} dx \mathcal{P}(t^n, x) = q_i^n \qquad \mathcal{P}(t^n, x_{i+\frac{1}{2}}) = q_{i+\frac{1}{2}}^n$$

462 Inserting this polynomial in (2.5) and integrating it instead of the source yields  
463 the following quadrature formula:

464 (4.6) 
$$\frac{1}{\Delta t} \int_0^{\Delta t} dt \frac{1}{\Delta x} \int_{-\frac{\Delta x}{2}}^{\frac{\Delta x}{2}} dx q(t^n + t, x_i + x) =$$

465 
$$\bar{q}_i^n + \frac{1}{12} \left( -5(q_{i-\frac{1}{2}}^n + q_{i+\frac{1}{2}}^n) + q_{i-\frac{1}{2}}^{n+1} + q_{i+\frac{1}{2}}^{n+1} + 4(q_{i-\frac{1}{2}}^{n+\frac{1}{2}} + q_{i+\frac{1}{2}}^{n+\frac{1}{2}}) \right)$$

466 The weights can be depicted as

$t^{n+1}$	$\frac{1}{12}$	$\frac{1}{12}$
$t^{n+\frac{1}{2}}$	$\frac{4}{12}$	$\frac{4}{12}$
$t^n$	$-\frac{5}{12}$	$-\frac{5}{12}$
	$x_{i-\frac{1}{2}}$	$x_{i+\frac{1}{2}}$

468 Again, the box indicates that the corresponding weight refers to the cell average,  
469 whereas the others multiply point values.

470 The time levels  $(n, n + \frac{1}{2}, n + 1)$  contribute with weights  $(\frac{1}{6}, \frac{2}{3}, \frac{1}{6})$ , such that this  
471 quadrature formula is a modification of Simpson's rule in time. Note that it is not

472 possible to use terms proportional to  $x^3$ ,  $x^2t$  or  $t^3$  instead of the term  $xt^2$  in the  
 473 polynomial ansatz, as then the system (4.3)–(4.5) does not admit a solution. In a  
 474 sense this is therefore the only choice of a simple quadrature formula.

475 Quadrature formula (4.6) can be used immediately in order to approximate (2.5)  
 476 for linear source terms.

477 **4.1.2. Nonlinear source term.** For nonlinear  $s$ , the average

$$478 \quad (4.7) \quad \int_{x_{i-\frac{1}{2}}}^{x_{i+\frac{1}{2}}} dx s(q(t^n, x))$$

480 in general is different from

$$481 \quad (4.8) \quad s \left( \int_{x_{i-\frac{1}{2}}}^{x_{i+\frac{1}{2}}} dx q(t^n, x) \right)$$

483 Point values, however, do not present any difficulties: one can just evaluate  $s$  on  
 484 them. Therefore we suggest to consider a reconstruction  $q_{\text{recon},i}(x)$  that interpolates  
 485  $q_{i-\frac{1}{2}}^n$  and  $q_{i+\frac{1}{2}}^n$  and whose average agrees with  $\bar{q}_i^n$ . It is computed anyway in order  
 486 to update the point values in time, see equation (2.7). This reconstruction can be  
 487 easily evaluated at the midpoint of the cell. Then, instead of the cell averages, one  
 488 works with a seventh point value  $q_{\text{recon},i}(0) = \frac{1}{4}(6\bar{q}_i^n - q_{i-\frac{1}{2}}^n - q_{i+\frac{1}{2}}^n)$ . Of course, this is  
 489 equivalent to replacing the average by a Simpson's rule in the quadrature, and thus  
 490 the order of the quadrature is not reduced. Therefore when using only point values  
 491 (the 6 pointwise degrees of freedom and one value at the cell midpoint) the weights  
 492 of the quadrature formula read

$t^{n+1}$	$\frac{1}{12}$	$\frac{1}{12}$
$t^{n+\frac{1}{2}}$	$\frac{4}{12}$	$\frac{4}{12}$
$t^n$	$-\frac{3}{12}$	$\frac{8}{12}$
	$x_{i-\frac{1}{2}}$	$x_{i+\frac{1}{2}}$

494 Equation (2.5) then is replaced by the quadrature

$$495 \quad (4.9) \quad \hat{s}_i = \frac{s(q_{i-\frac{1}{2}}^{n+1}) + s(q_{i+\frac{1}{2}}^{n+1}) + 4(s(q_{i-\frac{1}{2}}^{n+1}) + s(q_{i+\frac{1}{2}}^{n+1})) - 3(s(q_{i-\frac{1}{2}}^{n+1}) + s(q_{i+\frac{1}{2}}^{n+1})) + 8q_{\text{recon},i}(0))}{12}$$

497 This quadrature can now be used for nonlinear  $s$ . As (4.9) uses a Simpson quadrature  
 498 instead of the average, upon usage of a linear source  $s$ , it reduces to the expression  
 499 (4.6) because of the quadratic reconstruction.

500 If the source term vanishes, the scheme becomes conservative in the sense that  
 501 averages are updated using numerical fluxes.

## 502 4.2. Two spatial dimensions.

503 **4.2.1. Linear source term.** Similarly consider the setup of the active flux  
 504 method on two-dimensional Cartesian grids as described in 2.1. The available de-

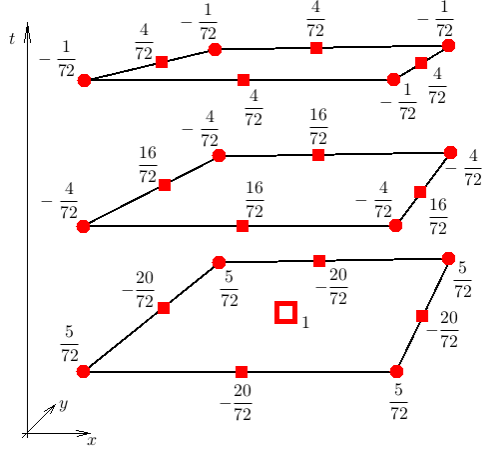


FIG. 3. Illustration of the weights of the space time quadrature formula (4.15).

505 grees of freedom are

506 (4.10)  $3 \times 4$  nodes:  $q_{i\pm\frac{1}{2},j\pm\frac{1}{2}}^n, q_{i\pm\frac{1}{2},j\pm\frac{1}{2}}^{n+\frac{1}{2}}, q_{i\pm\frac{1}{2},j\pm\frac{1}{2}}^{n+1}$

507 (4.11)  $3 \times 2$  vertical edges:  $q_{i\pm\frac{1}{2},j}^n, q_{i\pm\frac{1}{2},j}^{n+\frac{1}{2}}, q_{i\pm\frac{1}{2},j}^{n+1}$

508 (4.12)  $3 \times 2$  horizontal edges:  $q_{i,j\pm\frac{1}{2}}^n, q_{i,j\pm\frac{1}{2}}^{n+\frac{1}{2}}, q_{i,j\pm\frac{1}{2}}^{n+1}$

509 (4.13) 1 average:  $\bar{q}_{ij}^n$

511 The ansatz for a space-time polynomial is

512 (4.14) 
$$\mathcal{P}(t, x, y) = \left( \sum_{\zeta+\eta+\vartheta \leq 4} a_{\zeta\eta\vartheta} \cdot x^\zeta y^\eta t^\vartheta \right) + a_{212} x^2 y t^2 + a_{122} x y^2 t^2$$

513

514 It admits a unique solution to the interpolation problem given the available de-  
515 grees of freedom and yields the following quadrature formula (see also figure 3):

$$\begin{aligned} & \frac{1}{\Delta x} \int_{-\frac{\Delta x}{2}}^{\frac{\Delta x}{2}} dx \frac{1}{\Delta y} \int_{-\frac{\Delta y}{2}}^{\frac{\Delta y}{2}} dy \frac{1}{\Delta t} \int_0^{\Delta t} dt q(t, x, y) = \bar{q}_{ij}^n \\ & - \frac{20}{72} (q_E^n + q_N^n + q_S^n + q_W^n) + \frac{5}{72} (q_{NE}^n + q_{NW}^n + q_{SE}^n + q_{SW}^n) \\ & + \frac{16}{72} (q_E^{n+\frac{1}{2}} + q_N^{n+\frac{1}{2}} + q_S^{n+\frac{1}{2}} + q_W^{n+\frac{1}{2}}) - \frac{4}{72} (q_{NE}^{n+\frac{1}{2}} + q_{NW}^{n+\frac{1}{2}} + q_{SE}^{n+\frac{1}{2}} + q_{SW}^{n+\frac{1}{2}}) \\ & + \frac{4}{72} (q_E^{n+1} + q_N^{n+1} + q_S^{n+1} + q_W^{n+1}) - \frac{1}{72} (q_{NE}^{n+1} + q_{NW}^{n+1} + q_{SE}^{n+1} + q_{SW}^{n+1}) \end{aligned}$$

516 (4.15)

517

518 The time levels  $(n, n + \frac{1}{2}, n + 1)$  contribute again with weights  $(\frac{1}{6}, \frac{2}{3}, \frac{1}{6})$ , and the edges  
519 always contribute  $-4$  times the nodes.

520 **4.2.2. Nonlinear source term.** Again, for nonlinear source instead of the av-  
521 erage it is necessary to use the evaluation of the reconstruction at the cell midpoint.

522 This amounts to an approximation of the average by a two-dimensional Simpson rule.  
 523 Then the source term is approximating as follows:

$$\begin{aligned}
 & \frac{1}{\Delta x} \int_{-\frac{\Delta x}{2}}^{\frac{\Delta x}{2}} dx \frac{1}{\Delta y} \int_{-\frac{\Delta y}{2}}^{\frac{\Delta y}{2}} dy \frac{1}{\Delta t} \int_0^{\Delta t} dt s(q(t, x, y)) = \frac{32}{72} s(q_{\text{recon}, ij}(0, 0)) \\
 & - \frac{12}{72} (s(q_E^n) + s(q_N^n) + s(q_S^n) + s(q_W^n)) \\
 & + \frac{3}{72} (s(q_{NE}^n) + s(q_{NW}^n) + s(q_{SE}^n) + s(q_{SW}^n)) \\
 524 \quad (4.16) \quad & + \frac{16}{72} \left( s(q_E^{n+\frac{1}{2}}) + s(q_N^{n+\frac{1}{2}}) + s(q_S^{n+\frac{1}{2}}) + s(q_W^{n+\frac{1}{2}}) \right) \\
 & - \frac{4}{72} \left( s(q_{NE}^{n+\frac{1}{2}}) + s(q_{NW}^{n+\frac{1}{2}}) + s(q_{SE}^{n+\frac{1}{2}}) + s(q_{SW}^{n+\frac{1}{2}}) \right) \\
 & + \frac{4}{72} (s(q_E^{n+1}) + s(q_N^{n+1}) + s(q_S^{n+1}) + s(q_W^{n+1})) \\
 & - \frac{1}{72} (s(q_{NE}^{n+1}) + s(q_{NW}^{n+1}) + s(q_{SE}^{n+1}) + s(q_{SW}^{n+1}))
 \end{aligned}$$

525

526 In case that the data only depend on one of the variables, the two-dimensional  
 527 quadratures (4.15) and (4.16) do *not* exactly reduce to the one dimensional quadra-  
 528 tures (4.6) and (4.9). This is because (cf. Figure 3) the point values on edge midpoints  
 529  $(0, \pm \frac{\Delta y}{2})$  do not disappear even if the data depend only on  $x$ , and therefore the avail-  
 530 able degrees of freedom remain different from the one-dimensional case.

531

## 5. Well-balanced property for acoustics with gravity.

532

533 **5.1. Exact evolution operator.** As described in 3.2 a closed-form exact evo-  
 534 lution operator for acoustics with gravity is very difficult to obtain. Nevertheless,  
 535 it is still possible to show that a scheme endowed with such an operator would be  
 536 well-balanced / stationarity preserving; i.e. that there exists a discretization of the  
 537 stationary states of the PDE which remain exactly stationary. This proof does not  
 538 require the evolution operator to be known explicitly, but only relies on the fact that  
 539 it is exact. Besides its fundamental importance, this result is used in section 5.2  
 540 to analyze the situation for the approximate evolution operator and to restore the  
 541 well-balanced property for it.

542

543 The numerical stationary states are best studied upon the (discrete) Fourier trans-  
 544 form. Define  $t_x := \exp(\mathfrak{i}k_x \Delta x)$ ,  $t_y := \exp(\mathfrak{i}k_y \Delta y)$ . Here  $\mathfrak{i}$  is the imaginary unit and  
 545  $\mathbf{k} = (k_x, k_y) \in \mathbb{R}^2$  is the wave vector characterizing the spatial frequency of the Fourier  
 546 mode. Applying the Fourier transform introduces one mode  $\bar{q}$  for the averages and  
 547 one mode  $q$  for the point values; this implies writing  $q_i := \bar{q}^i t_x^i t_y^j$ ,  $q_{i+\frac{1}{2}} := q^i t_x^i t_y^j$ .

548

549 **THEOREM 5.1** (Stationarity preservation with exact evolution). *If the discrete*

550

551 *data fulfill*

$$\begin{aligned}
 548 \quad (5.1) \quad & \bar{\rho}_i = \frac{\rho_{i+\frac{1}{2}} + \rho_{i-\frac{1}{2}}}{2} \\
 549 \quad (5.2) \quad & \frac{p_{i+\frac{1}{2}} - p_{i-\frac{1}{2}}}{\Delta x} = g \frac{\rho_{i-\frac{1}{2}} + \rho_{i+\frac{1}{2}}}{2} \\
 550 \quad (5.3) \quad & \frac{\bar{p}_{i+\frac{3}{2}} - \bar{p}_{i+\frac{1}{2}}}{\Delta x} = g \frac{\rho_{i+\frac{3}{2}} + 4\rho_{i+\frac{1}{2}} + \rho_{i-\frac{1}{2}}}{6}
 \end{aligned}$$

551

552 *and the exact evolution operator for (3.6)–(3.8) is used, then the numerical solution*  
 553 *remains stationary.*



554 *Proof.* The proof consists of two parts.

555 i) Consider first the evolution of the point values. When the exact evolution opera-  
 556 tor is used to update the point values, they remain stationary if the reconstruction  
 557 fulfills

$$558 \quad (5.4) \quad v_{\text{recon}}(x) = \text{const} \quad \partial_x p_{\text{recon}}(x) = \rho_{\text{recon}}(x)g$$

560 Upon the Fourier transform this becomes (w.l.o.g.  $x_i = 0$ )

$$561 \quad (5.5) \quad -3 \left( 2\bar{p} - p \left( 1 + \frac{1}{t_x} \right) \right) \frac{2x}{\Delta x^2} + p \left( 1 - \frac{1}{t_x} \right) \frac{1}{\Delta x} =$$

$$562 \quad (5.6) \quad -3g \left( 2\bar{p} - \rho \left( 1 + \frac{1}{t_x} \right) \right) \frac{x^2}{\Delta x^2} + g\rho \left( 1 - \frac{1}{t_x} \right) \frac{x}{\Delta x} + g \frac{6\bar{p} - \rho \left( 1 + \frac{1}{t_x} \right)}{4}$$

564 This shall be valid for all  $x$ :

$$565 \quad (5.7) \quad 2\bar{p} - \rho(1 + 1/t_x) = 0$$

$$566 \quad (5.8) \quad -2\bar{p}t_x + p(t_x + 1) = \frac{\Delta x g \rho (t_x - 1)}{6}$$

$$567 \quad (5.9) \quad p(t_x - 1) = \Delta x g \frac{6\bar{p}t_x - \rho(t_x + 1)}{4}$$

569 These are three equations for four variables. In particular

$$570 \quad (5.10) \quad \bar{\rho} = \frac{\rho(1 + 1/t_x)}{2}$$

$$571 \quad (5.11) \quad p = \Delta x g \rho \frac{t_x + 1}{2(t_x - 1)}$$

$$572 \quad (5.12) \quad \bar{p} = \Delta x g \rho \frac{t_x^2 + 4t_x + 1}{6t_x(t_x - 1)}$$

574 These statements can be rewritten as finite difference formulae by inverting the  
 575 Fourier transform:

$$576 \quad (5.13) \quad \bar{\rho} = \frac{\rho_{i+\frac{1}{2}} + \rho_{i-\frac{1}{2}}}{2}$$

$$577 \quad (5.14) \quad \frac{p_{i+\frac{1}{2}} - p_{i-\frac{1}{2}}}{\Delta x} = g \frac{\rho_{i-\frac{1}{2}} + \rho_{i+\frac{1}{2}}}{2}$$

$$578 \quad (5.15) \quad \frac{\bar{p}_{i+1} - \bar{p}_i}{\Delta x} = g \frac{\rho_{i+\frac{3}{2}} + 4\rho_{i+\frac{1}{2}} + \rho_{i-\frac{1}{2}}}{6}$$

580 ii) Assume now (5.10)–(5.12) to be true. Simpson’s rule in time for the flux average  
 581 is trivial, and thus the update of the cell average amounts to

$$582 \quad (5.16) \quad \frac{\bar{v}^{n+1} - \bar{v}^n}{\Delta t} + \frac{p(1 - 1/t_x)}{\Delta x} = \frac{\bar{v}^{n+1} - \bar{v}^n}{\Delta t} + g\rho \frac{t_x + 1}{2t_x}$$

$$583 \quad (5.17) \quad = \frac{\bar{v}^{n+1} - \bar{v}^n}{\Delta t} + g\bar{\rho} \quad \square$$

585 The quadrature formula (4.6) for the source reduces to  $g\bar{\rho}$  if the point values are  
 586 stationary, which implies  $\bar{v}^{n+1} = \bar{v}^n$ . This completes the proof.

587 The equations (5.10)–(5.12) contain  $\rho$  as a free variable. One can rewrite the  
588 system making  $p$  the free variable:

$$589 \quad (5.18) \quad \bar{\rho} = \frac{p(t_x - 1)}{t_x \Delta x g} \quad \rho = \frac{2p(t_x - 1)}{\Delta x g(t_x + 1)} \quad \bar{p} = p \frac{t_x^2 + 4t_x + 1}{3t_x(t_x + 1)}$$

591 This form will be useful later.

592 Equations (5.2)–(5.3) are finite difference approximations of  $\partial_x p = \rho g$ . Equation  
593 (5.1) implies that the reconstructed  $\rho$  of the discrete stationary state is linear, which  
594 is clear: for quadratic reconstructions to fulfill (5.4),  $\rho_{\text{recon}}$  has to be linear in each  
595 cell. The slope of the linear function can vary from cell to cell and is given by (5.2).

596 **5.2. Approximate evolution operator.** The above section identifies condi-  
597 tions (5.1)–(5.3) on the discrete data for them to remain stationary upon usage of the  
598 *exact* evolution operator. Unfortunately, such an operator is unavailable in practice.  
599 Having identified an approximate solution operator, which agrees with the exact so-  
600 lution up to terms  $\mathcal{O}(t^3)$  in section 3.3, here we study whether it keeps the same data  
601 (5.1)–(5.3) stationary as well.

602 **THEOREM 5.2.** *If the discrete data fulfill (5.1)–(5.3) and the approximate evolu-*  
603 *tion operator of theorem 3.2 for (3.6)–(3.8) is used, then both the pressure  $p$  and the*  
604 *density  $\rho$  remain stationary over one time step, but the velocity undergoes the time*  
605 *evolution*

$$606 \quad (5.19) \quad v_{i+\frac{1}{2}}(t) = -\frac{\alpha g^2}{4} \frac{\rho_{i+\frac{1}{2}} - \rho_{i-\frac{1}{2}}}{\Delta x} t^3$$

608 *Proof.* Assume the initial data to fulfill (5.1)–(5.3), or equivalently (5.4). Using  
609 (2.7) (and applying the discrete Fourier transform straight away) (5.4) implies

$$610 \quad (5.20) \quad p_{\text{recon}}(x) = \frac{1}{4} \left( 6\bar{p} - p \left( 1 + \frac{1}{t_x} \right) \right) + \frac{x}{\Delta x} \left( 1 - \frac{1}{t_x} \right) p - 3 \frac{x^2}{\Delta x^2} \left( 2\bar{p} - p \left( 1 + \frac{1}{t_x} \right) \right)$$

$$611 \quad (5.21) \quad \rho_{\text{recon}}(x) = \frac{1}{g \Delta x} \left( p \left( 1 - \frac{1}{t_x} \right) - 6 \frac{x}{\Delta x} \left( 2\bar{p} - p \left( 1 + \frac{1}{t_x} \right) \right) \right)$$

$$612 \quad (5.22) \quad v_{\text{recon}}(x) = 0$$

614 and using (3.44) therefore

$$615 \quad (5.23) \quad Q_{1,0}(x) = Q_{2,0}(x) = -\frac{p(1+t_x) - 6\bar{p}t_x}{8t_x} + \frac{p(t_x-1)x}{2\Delta xt_x} + \frac{3(p(1+t_x) - 2\bar{p}t_x)x^2}{2\Delta x^2 t_x}$$

$$616 \quad (5.24) \quad Q_{3,0}(x) = \frac{p(-1+t_x)}{\Delta x g t_x} + \frac{p - 6\bar{p}t_x + p t_x}{4c^2 t_x} \\ 617 \quad + \frac{(-\Delta x g p(t_x - 1) + 6c^2(p(1+t_x) - 2\bar{p}t_x))x}{c^2 \Delta x^2 g t_x} - \frac{3(p(1+t_x) - 2\bar{p}t_x)x^2}{c^2 \Delta x^2 t_x}$$

619 Evaluating the Runge-Kutta algorithm of section 3.3 on these initial data (at

620  $x = \frac{\Delta x}{2}$ ) yields

$$621 \quad (5.25) \quad \begin{pmatrix} \rho \\ v^* \\ p \end{pmatrix} \quad \text{with} \quad v^* = -\frac{\alpha g(t_x - 1)^2}{2\Delta x^2 t_x(t_x + 1)} p t^3$$

622 ( $\alpha$  is the parameter appearing in the RK2 method.)

624 Recall that  $\rho$  and  $p$  are the Fourier coefficients of the point values of the density  
 625 and the pressure. Obviously  $\rho$  and  $p$  remain stationary, but the velocity does not.  
 626 Using (5.18)  $v^*$  can be rewritten as

$$627 \quad (5.26) \quad v^* = -\frac{\alpha g^2}{4\Delta x} \left(1 - \frac{1}{t_x}\right) \rho t^3 = -\frac{\alpha g^2}{4} \frac{\rho_{i+\frac{1}{2}} - \rho_{i-\frac{1}{2}}}{\Delta x} t^3$$

629 having applied the inverse Fourier transform in the last step.  $\square$

630 Observe that the time evolution of the velocity is consistent with the accuracy of  
 631 the algorithm ( $\mathcal{O}(t^3)$ ).

632 COROLLARY 5.3 (Stationarity preservation with approximate evolution). *If the*  
 633 *algorithm of section 3.3 is modified by adding the term*

$$634 \quad (5.27) \quad \frac{\alpha g^2}{4} \frac{\rho_{i+\frac{1}{2}} - \rho_{i-\frac{1}{2}}}{\Delta x} t^3$$

636 *to the velocity evolution, then*

637 *i) its accuracy is not changed*

638 *ii) it becomes stationarity preserving / well-balanced with the same discrete station-*  
 639 *ary states as the exact evolution operator*

640 The two forms (5.25) and (5.19) of  $v^*$  are equivalent, because the initial data  
 641 have been chosen to be stationary, and thus additionally fulfill (5.18). The proposed  
 642 modification is to *always* add  $-v^*$  to the velocity evolution, irrespective of whether  
 643 the data fulfill (5.18) or not. At this point the Fourier coefficients of  $\rho$  and  $p$  are  
 644 independent and it matters whether the correction is used in the form (5.25) or (5.19).  
 645 Of course, also the inverse Fourier transform has to be applied to the expression first  
 646 in order for the correction to attain the form of a finite difference formula. Compact  
 647 finite difference formulae are in one-to-one-correspondence with Laurent polynomials  
 648 in  $t_x$ . An expression such as  $\frac{1}{t_x+1} = 1 - t_x + t_x^2 \mp \dots$  is an expression involving an  
 649 unbounded stencil and cannot be implemented in usual codes. Therefore (5.19) cannot  
 650 be used as a correction because the correction would have a non-compact stencil (just  
 651 as the equivalent expressions involving only  $\bar{\rho}$  or  $\bar{p}$ ). This is why the form (5.25) which  
 652 involves point values of  $\rho$  is preferred.

653 Being always present in the velocity evolution (and not only at stationary states),  
 654 the modification (5.27) might in general affect the stability of the algorithm, but it  
 655 has not been found to have any effect on the stability in practice.

656 **6. Numerical examples.** The numerical examples of this section serve to il-  
 657 lustrate the performance of the new method. The equations discussed are linear  
 658 advection with different source terms (in one and two spatial dimensions, as intro-  
 659 duced in section 3.1) and linear acoustics with gravity (introduced in section 3.2). In  
 660 both cases it is demonstrated that the method achieves third order of accuracy in the  
 661 experiments. For acoustics with gravity additionally the discrete stationary states are  
 662 studied and shown to agree with the prediction of section 5.

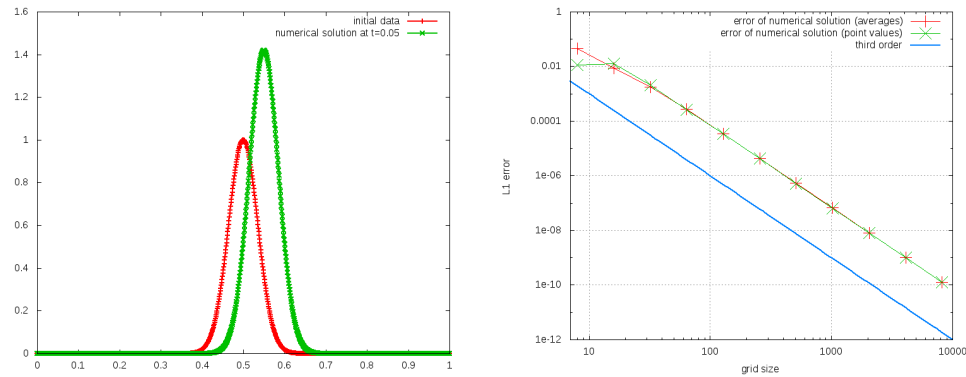


FIG. 4. Gaussian initial data for (6.1) with  $\mathbf{U} = \mathbf{e}_x$ ,  $\kappa = 7$ . Note that due to the source term, the Gaussian is advected and also changes shape. Exact evolution operator (3.4) and quadrature formula (4.6) have been used with  $CFL = 0.45$ . Left: Initial data and solution at  $t = 0.05$  (cell averages) on a grid with 1000 cells. Right: Error of the numerical solution as a function of the grid size shows third order convergence.

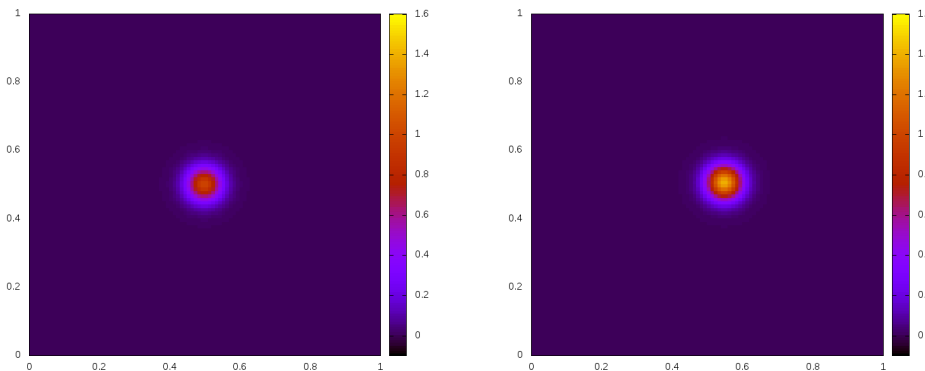


FIG. 5. Gaussian initial data for (6.1) with  $\mathbf{U} = (1, 0.1)$ ,  $\kappa = 7$ . Note that due to the source term, the Gaussian is advected and also changes shape. Exact evolution operator (3.4) and quadrature formula (4.15) have been used with  $CFL = 0.45$ . Left: Initial setup. Right: Numerical solution at  $t = 0.05$  on a  $100 \times 100$  Cartesian grid.

663 **6.1. Linear advection.** Consider first

$$664 \quad (6.1) \quad \partial_t q + \mathbf{U} \cdot \nabla q = \kappa q$$

666 with the exact solution given by (3.4). In Figures 4–6 the exact solution operator is  
 667 used for the evolution of the point values and third order convergence is observed. This  
 668 shows that the quadrature formulae (4.6) and (4.15) used to evolve the cell averages  
 669 indeed yield a third order scheme. Figure 4 shows the setup for a one-dimensional  
 670 situation together with a convergence study, Figure 5 shows the setup in two spatial  
 671 dimensions and Figure 6 shows the corresponding convergence study.

672 Consider now

$$673 \quad (6.2) \quad \partial_t q + \mathbf{U} \cdot \nabla q = \kappa q^B \quad B \neq 1$$

675 with the exact solution (3.5) and  $\kappa = 7$ ,  $B = 3$ . Figure 7 (left) shows the initial  
 676 data and the numerical solution, and Figure 7 (right) shows a convergence study for

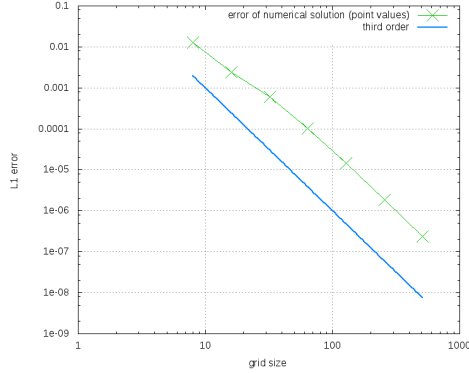


FIG. 6. Convergence study for the setup shown in Figure 5. One observes third order accuracy.

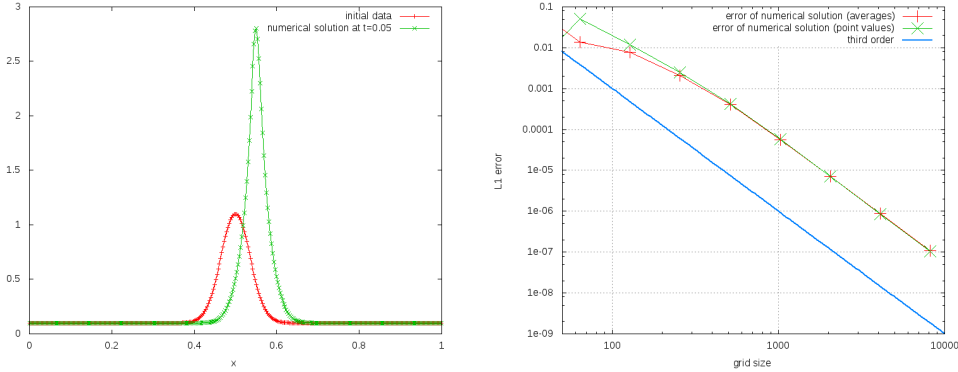


FIG. 7. Gaussian initial data for (6.2) with  $s(q) = \kappa q^B$  and  $\mathbf{U} = \mathbf{e}_x$ ,  $\kappa = 7$ ,  $B = 3$ . Runge-Kutta approximate evolution operator from Corollary 3.4 and quadrature formula (4.9) have been used with  $CFL = 0.45$ . The solution has been computed on a grid covering  $[-1 : 2]$ , but the error is only computed inside  $[0, 1]$  to exclude any boundary influence. Left: Initial setup and solution at  $t = 0.05$  (point values) on a grid with 1000 cells. Right: Error of the numerical solution as a function of the grid size shows third order convergence. The exact solution is given by (3.5).

677 the approximate evolution operator from Corollary (3.4). One observes third order  
 678 accuracy, as expected.

679 **6.2. Acoustics with gravity.** Consider now the equations of linear acoustics  
 680 with a gravity source term (3.6)–(3.8). The exact solution operator is only partly  
 681 available in closed form, and therefore the approximate Runge-Kutta evolution op-  
 682 erator of section 3.3 is used in combination with the well-balancing fix (5.27). The  
 683 parameter  $\alpha$  in the Runge-Kutta method is chosen to  $\alpha = \frac{1}{2}$ .

684 Figure 8 shows a stationary setup given by

685 (6.3) 
$$p = A_1 x^2 + A_2 x + A_3 \quad \rho = 2A_1 x/g + A_2/g \quad v = 0$$

687 with  $A_1 = 17, A_2 = -3, A_3 = 1$ . This parabola is exactly recovered by the reconstruc-  
 688 tion, and thus remains stationary up to machine precision. This experiment shows  
 689 that the well-balancing fix works as it should.

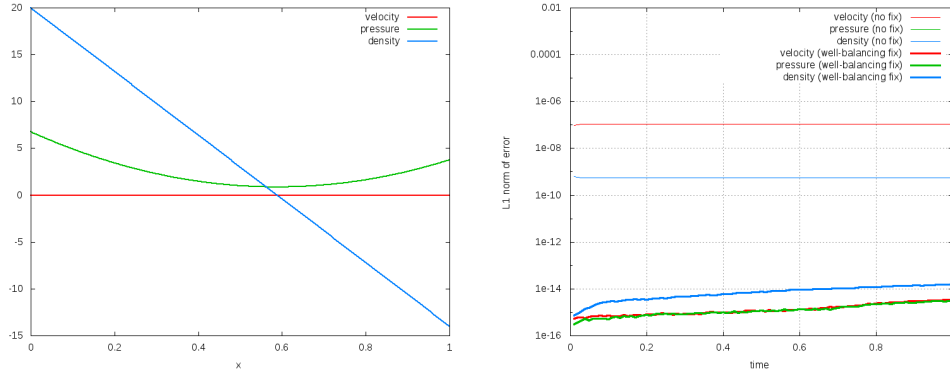


FIG. 8. Setup of a stationary parabola (6.3) for (3.6)–(3.8), solved using the Runge-Kutta approximate evolution operator of section 3.3 with and without well-balancing (5.27). Here  $g = -1$ , and the setup is solved on a grid covering  $[-1.5, 2.5]$ , but the error is only measured inside  $[0, 1]$  ( $\Delta x = 10^{-2}$ ) to exclude the influence of the boundaries. Left: Setup. Right: Error of numerical solution as a function of time. Thin lines: without the well-balancing (5.27). Thick lines: including the well-balancing (5.27). In the latter case one only observes an evolution due to machine error.

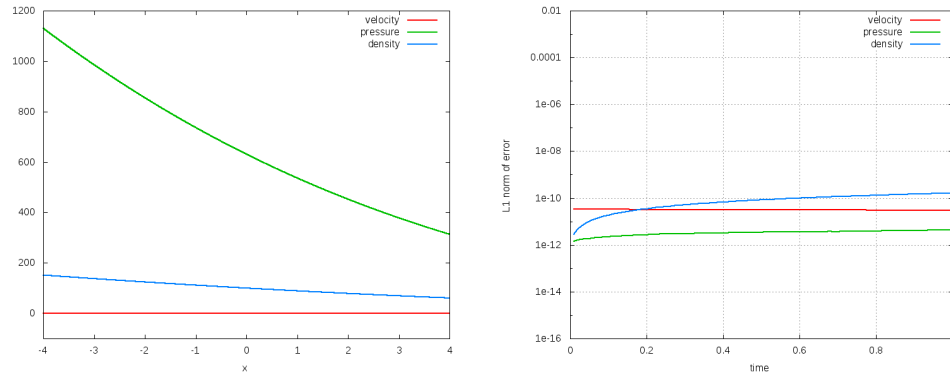


FIG. 9. Stationary setup (6.4) for (3.6)–(3.8), solved using the Runge-Kutta approximate evolution operator of section 3.3 with well-balancing (5.27). Here  $g = -1$ , and the setup is solved on a grid covering  $[-5.5, 5.5]$ , but the error is only measured inside  $[-4, 4]$  ( $\Delta x = 10^{-3}$ ) to exclude the influence of the boundaries. Left: Setup (cell averages). Right: Error of numerical solution as a function of time. One observes a transition towards a numerical stationary state which then persists forever.

690 Consider next (Figure 9) the stationary setup fulfilling  $p = K\rho^\gamma$ , i.e.

691 (6.4) 
$$\rho = \left( \frac{g(\gamma - 1)}{K\gamma} x + \rho_0^{\gamma-1} \right)^{\frac{1}{\gamma-1}}$$

692

693 with  $K = 1, \gamma = 1.4, \rho_0 = 100$ . This is reminiscent of an isentropic atmosphere  
 694 in the context of the Euler equations. This setup is not recovered exactly by the  
 695 reconstruction, but one observes a numerical evolution towards a discrete stationary  
 696 state which then persists forever.

697 Next, a perturbation

698 (6.5) 
$$200 \exp(-100x^2)$$

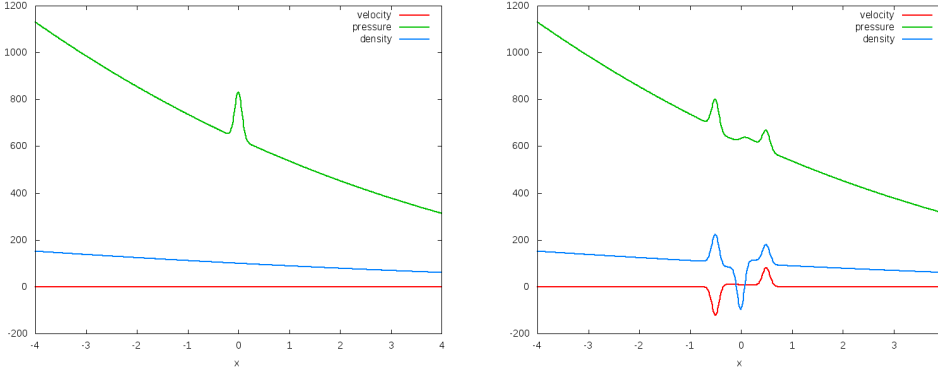


FIG. 10. Setup (6.4) endowed with the pressure perturbation (6.5) solved using the Runge-Kutta approximate evolution operator of section 3.3 with well-balancing (5.27). Left: Initial data (cell averages). Right: Numerical solution (cell averages) at  $t = 0.5$  on a grid covering  $[-5.5, 5.5]$ , but only the subinterval  $[-4, 4]$  is considered in order to exclude the influence of the boundaries.  $\Delta x = 0.01$ ,  $CFL = 0.45$ .

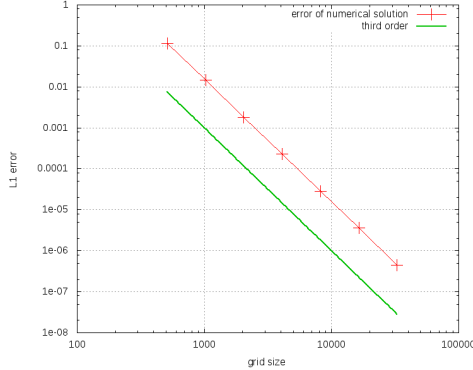


FIG. 11. Setup of Figure 10. The error of the numerical solution is measured on the point values. One observes third order accuracy.

700 in the pressure is added onto the setup (6.4). In order to study the accuracy of the  
 701 scheme on this setup, it is solved on a grid of  $131072 = 2^{18}$  cells and the solution is  
 702 used as reference. Again,  $g = -1, K = 1, \gamma = 1.4$ . Figure 10 shows the setup and  
 703 the numerical solution at  $t = 0.5$ , and Figure 11 shows a convergence study which  
 704 displays third order convergence.

705 Consider finally a Riemann problem:

$$706 \quad (6.6) \quad \rho = 3.5 \quad p = 1.5 \quad v = \begin{cases} 1 & 0.25 \leq x \leq 0.75 \\ 3 & \text{else} \end{cases}$$

708 This Riemann problem can be solved exactly using the formula (A.18)–(A.22). Note  
 709 that if all quantities are constant in space, then they solve

$$710 \quad (6.7) \quad \partial_t \rho = 0$$

$$711 \quad (6.8) \quad \partial_t p = 0$$

$$712 \quad (6.9) \quad \partial_t v = \rho g$$

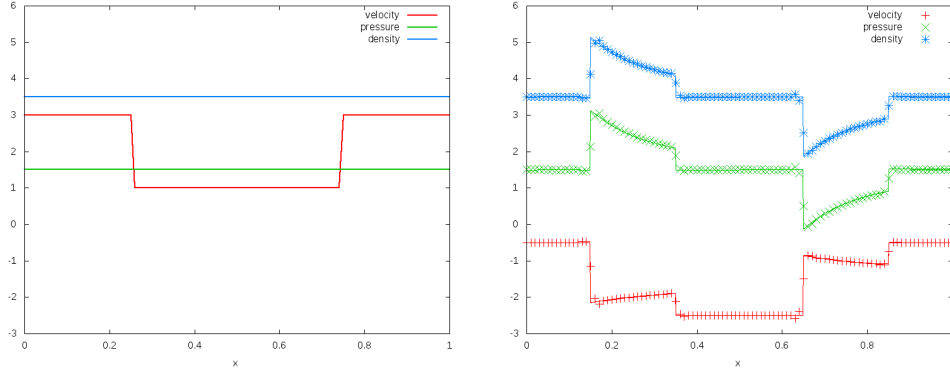


FIG. 12. Riemann problem setup (6.6) solved using the Runge-Kutta approximate evolution operator of section 3.3 with well-balancing (5.27). Here,  $g = -10$ . Left: Initial data. Right: Numerical solution (dots) and exact solution (solid line) at  $t = 0.1$ .  $\Delta x = 0.01$ ,  $CFL = 0.45$ . Point values of the numerical solution are shown.

714 which means that  $\rho$  and  $p$  remain stationary, but that  $v = v(t = 0) + \rho gt$ . The solution  
 715 to the initial data (6.6) therefore can be obtained by adding the time evolution of

716  $\begin{pmatrix} 0 \\ v_0(x) \\ 0 \end{pmatrix}$  (via numerical quadrature of (A.18)–(A.22)) and the time evolution of  
 717  $\begin{pmatrix} \rho \\ 0 \\ p \end{pmatrix}$  which is just  $\begin{pmatrix} \rho \\ \rho gt \\ p \end{pmatrix}$ . Figure 12 shows the numerical and the exact solution.

718 **7. Conclusions and outlook.** Active flux is a novel kind of numerical method  
 719 for hyperbolic problems, extending the finite volume method. Instead of computing  
 720 the intercell flux via a Riemann problem it relies on a continuous reconstruction and on  
 721 accurately evolved point values along the cell boundary. They then immediately serve  
 722 as quadrature values for the computation of the intercell flux. The extension of active  
 723 flux to time dependent balance laws presented in this paper requires a modification  
 724 in both these aspects: the evolution of the point values and the average update  
 725 need to account for the source term. Here, an approximate evolution operator is  
 726 suggested for the point value update; this is done for linear systems with possibly  
 727 nonlinear source terms in one spatial dimension, and linear scalar equations with  
 728 source terms in multiple spatial dimensions. A suitable quadrature is suggested in  
 729 order to approximate the contribution of the source term to the cell average. This  
 730 quadrature can be applied to any system of (nonlinear) balance laws.

731 We aim at combining the strategy presented in this paper with an approximate  
 732 evolution operator for a nonlinear homogeneous problem (such as those suggested  
 733 in [Bar19a]) in future. Multi-dimensional systems of hyperbolic conservation laws  
 734 are very different from their one-dimensional counterparts because in general char-  
 735 acteristics are unavailable and need to be conceptually replaced by characteristic  
 736 cones. Examples of evolution operators that make use of such cones can be found in  
 737 [ER13, FR15, Fan17, BHKR19]. Combining these with an approximate evolution of



738 the source term shall pave the way towards the extension of active flux to nonlinear  
 739 multi-dimensional balance laws and the derivation of accurate structure preserving  
 740 (in particular well-balanced) methods for them.

741 **Appendix A. Exact solution of linear acoustics with gravity.**

742 System (3.6)–(3.8) can in principle be immediately solved exactly via Fourier  
 743 transform by inserting the ansatz

$$744 \quad (\text{A.1}) \quad \begin{pmatrix} \rho \\ v \\ p \end{pmatrix} = \begin{pmatrix} \hat{\rho} \\ \hat{v} \\ \hat{p} \end{pmatrix} \exp(\mathfrak{i}k \cdot x - \mathfrak{i}\omega t)$$

745  
 746 into (3.6)–(3.8):

$$747 \quad (\text{A.2}) \quad \omega \begin{pmatrix} \hat{\rho} \\ \hat{v} \\ \hat{p} \end{pmatrix} = \begin{pmatrix} 0 & k & 0 \\ \mathfrak{i}g & 0 & k \\ 0 & c^2k & 0 \end{pmatrix} \begin{pmatrix} \hat{\rho} \\ \hat{v} \\ \hat{p} \end{pmatrix}$$

748  
 749 Therefore  $\omega = 0$ , or  $\omega = \pm\sqrt{c^2k^2 + \mathfrak{i}gk}$ . The complex eigenvalue can be removed  
 750 upon transforming

$$751 \quad (\text{A.3}) \quad \rho = \tilde{\rho}e^{\mu x} \quad v = \tilde{v}e^{\mu x} \quad p = \tilde{p}e^{\mu x}$$

752 with

$$754 \quad (\text{A.4}) \quad \mu := \frac{g}{2c^2}$$

755  
 756 System (3.6)–(3.8) then reads

$$757 \quad (\text{A.5}) \quad \partial_t \tilde{\rho} + \partial_x \tilde{v} = -\mu \tilde{v}$$

$$758 \quad (\text{A.6}) \quad \partial_t \tilde{v} + \partial_x \tilde{p} = \tilde{\rho}g - \mu \tilde{p}$$

$$759 \quad (\text{A.7}) \quad \partial_t \tilde{p} + c^2 \partial_x \tilde{v} = -c^2 \mu \tilde{v}$$

760  
 761 Now, a solution of (A.5)–(A.7) shall be found. For better readability, drop the tilde.

762 Upon the Fourier transform (A.5)–(A.7) becomes

$$763 \quad (\text{A.8}) \quad \omega \begin{pmatrix} \hat{\rho} \\ \hat{v} \\ \hat{p} \end{pmatrix} = \mathcal{E} \begin{pmatrix} \hat{\rho} \\ \hat{v} \\ \hat{p} \end{pmatrix} \quad \mathcal{E} = \begin{pmatrix} 0 & k - \mathfrak{i}\mu & 0 \\ \mathfrak{i}g & 0 & k - \mathfrak{i}\mu \\ 0 & c^2k - \mathfrak{i}c^2\mu & 0 \end{pmatrix}$$

764  
 765 The eigenvalues of  $\mathcal{E}$  are now real:  $\omega_1 = 0$ ,  $\omega_{2,3} = \pm c\sqrt{k^2 + \mu^2}$ . Although this  
 766 transformation brings the endeavour of finding the exact solution to (3.6)–(3.8) into  
 767 the realm of the possible, technical difficulties prevent one from actually computing  
 768 all Green's functions in closed form.

769 Assume therefore that the only non-vanishing initial data are in the velocity.

770 Then the Fourier mode at initial time reads

$$771 \quad (\text{A.9}) \quad \begin{pmatrix} 0 \\ \hat{v} \\ 0 \end{pmatrix} \exp(\mathfrak{i}kx)$$

772

773 and at a later time it becomes

$$774 \quad (\text{A.10}) \quad \sum_{m=1}^3 v_m \exp(\mathfrak{i}kx - \mathfrak{i}\omega_m t)$$

775  
776 where the decomposition of  $\begin{pmatrix} 0 \\ \hat{v} \\ 0 \end{pmatrix}$  in the eigenbasis of  $\mathcal{E}$  is used, i.e.

$$777 \quad (\text{A.11}) \quad \begin{pmatrix} 0 \\ \hat{v} \\ 0 \end{pmatrix} = \sum_{m=1}^3 v_m \quad \mathcal{E}v_m = \omega_m v_m$$

778

779 Such a basis is given e.g. by

$$780 \quad (\text{A.12}) \quad e_1 = \begin{pmatrix} \mu + \mathfrak{i}k \\ 0 \\ g \end{pmatrix} \quad e_{2,3} = \begin{pmatrix} \mu + \mathfrak{i}k \\ \pm \mathfrak{i}c\sqrt{k^2 + \mu^2} \\ c^2(\mu + \mathfrak{i}k) \end{pmatrix}$$

781

782 Collecting the terms yields the time evolution of the Fourier mode (A.9):

$$783 \quad (\text{A.13}) \quad \hat{v} \exp(\mathfrak{i}kx) \begin{pmatrix} -\frac{(\mu + \mathfrak{i}k) \sin(ct\sqrt{k^2 + \mu^2})}{c\sqrt{k^2 + \mu^2}} \\ \cos(ct\sqrt{k^2 + \mu^2}) \\ -\frac{c^2(\mu + \mathfrak{i}k) \sin(ct\sqrt{k^2 + \mu^2})}{c\sqrt{k^2 + \mu^2}} \end{pmatrix}$$

$$784 \quad (\text{A.14}) \quad = \hat{v} \begin{pmatrix} -(\mu + \partial_x) \\ \partial_t \\ -c^2(\mu + \partial_x) \end{pmatrix} \exp(\mathfrak{i}kx) \frac{\sin(ct\sqrt{k^2 + \mu^2})}{c\sqrt{k^2 + \mu^2}}$$

785

786 Green's function is obtained by inserting the Fourier transform of a Dirac  $\delta_{x'}$  at  
787  $x'$ , i.e. taking  $\hat{v} = \frac{\exp(-\mathfrak{i}kx')}{\sqrt{2\pi}}$  and performing the inverse Fourier transform with the  
788 help of formula 1.7 (30) in [Bat54]. This yields, wherever defined,

$$789 \quad (\text{A.15}) \quad \begin{pmatrix} G_\rho(t, x; x') \\ G_v(t, x; x') \\ G_p(t, x; x') \end{pmatrix} = \begin{pmatrix} -(\mu + \partial_x) \\ \partial_t \\ -c^2(\mu + \partial_x) \end{pmatrix} \frac{1}{2c} J_0\left(\mu\sqrt{(ct)^2 - (x - x')^2}\right)$$

$$790 \quad (\text{A.16}) \quad + \begin{pmatrix} -\frac{\delta_{x+ct} - \delta_{x-ct}}{2c} \\ \frac{\delta_{x+ct} + \delta_{x-ct}}{2} \\ c(\delta_{x+ct} - \delta_{x-ct}) \end{pmatrix}$$

791

792 where  $J_0$  is the 0-th order Bessel function of the first kind, and  $J'_0 = -J_1$ . Then the  
 793 solution is obtained by performing a convolution with the initial data. Reinstalling  
 794 the tilde one has

795 (A.17)  $\tilde{v}(t, x) = \int dx' G_v(t, x; x') \tilde{v}_0(x')$

796 (A.18)  $v(t, x) = \int dx' G_v(t, x; x') e^{\mu(x-x')} v_0(x')$

797 (A.19)  $= \frac{1}{2} \int dx' e^{\mu(x-x')} \partial_{ct} J_0 \left( \mu \sqrt{(ct)^2 - (x-x')^2} \right) v_0(x')$

798 (A.20)  $+ \frac{1}{2} \left( e^{-\mu ct} v_0(x+ct) + e^{\mu ct} v_0(x-ct) \right)$

799 (A.21)  $\rho(t, x) = -\frac{1}{2c} \int dx' e^{\mu(x-x')} (\mu + \partial_x) J_0 \left( \mu \sqrt{(ct)^2 - (x-x')^2} \right) v_0(x')$

800 (A.22)  $- \frac{1}{2c} \left( e^{-\mu ct} v_0(x+ct) - e^{\mu ct} v_0(x-ct) \right)$   
 801

802 and analogously for  $p$ . However, it is easier to note that

803 (A.23)  $\partial_t(c^2 \rho - p) = 0$

805 such that

806 (A.24)  $p(t, x) = p_0(x) + c^2 \left( \rho(t, x) - \rho_0(x) \right)$   
 807

808 **Acknowledgments.** We thank Philip L. Roe for valuable comments and advice.

809 REFERENCES

810 [ABB<sup>+</sup>04] Emmanuel Audusse, François Bouchut, Marie-Odile Bristeau, Rupert Klein, and Benoit  
 811 Perthame. A fast and stable well-balanced scheme with hydrostatic reconstruction  
 812 for shallow water flows. *SIAM Journal on Scientific Computing*, 25(6):2050–2065,  
 813 2004.

814 [Bar18] Wasilij Barsukow. *Low Mach number finite volume methods for the acoustic and Euler*  
 815 *equations*. Doctoral thesis, University of Wuerzburg, 2018.

816 [Bar19a] W Barsukow. The active flux scheme for nonlinear problems which admit characteristic  
 817 variables. *submitted to J. Sci. Comp*, 2019.

818 [Bar19b] Wasilij Barsukow. Stationarity preserving schemes for multi-dimensional linear systems.  
 819 *Mathematics of Computation*, 88(318):1621–1645, 2019.

820 [Bat54] Harry Bateman. *Tables of integral transforms (volume 1)*, volume 1. McGraw-Hill  
 821 Book Company, 1954.

822 [BCK16] Jonas P Berberich, Praveen Chandrashekar, and Christian Klingenberg. A general  
 823 well-balanced finite volume scheme for euler equations with gravity. In *XVI In-*  
 824 *ternational Conference on Hyperbolic Problems: Theory, Numerics, Applications*,  
 825 pages 151–163. Springer, 2016.

826 [BCK19] Jonas P Berberich, Praveen Chandrashekar, and Christian Klingenberg. High order  
 827 well-balanced finite volume methods for multi-dimensional systems of hyperbolic  
 828 balance laws. *arXiv preprint arXiv:1903.05154*, 2019.

829 [BCKR19] Jonas P Berberich, Praveen Chandrashekar, Christian Klingenberg, and Friedrich K  
 830 Röpke. Second order finite volume scheme for Euler equations with gravity which  
 831 is well-balanced for general equations of state and grid systems. *Communications*  
 832 *in Computational Physics*, 26:599–630, 2019.

833 [BHKR19] Wasilij Barsukow, Jonathan Hohm, Christian Klingenberg, and Philip L Roe. The  
 834 active flux scheme on Cartesian grids and its low Mach number limit. *Journal of*  
 835 *Scientific Computing*, 81(1):594–622, 2019.

836 [BKCK20] Jonas P Berberich, Roger Käppeli, Praveen Chandrashekar, and Christian Klingenberg.  
 837 High order discretely well-balanced finite volume methods for Euler equations with

- 838 gravity – without any a priori information about the hydrostatic solution. *arXiv*  
839 *preprint arXiv:2005.01811*, 2020.
- 840 [BV94] Alfredo Bermudez and Ma Elena Vázquez. Upwind methods for hyperbolic conservation  
841 laws with source terms. *Computers & Fluids*, 23(8):1049–1071, 1994.
- 842 [CCK<sup>+</sup>18] Alina Chertock, Shumo Cui, Alexander Kurganov, Şeyma Nur Özcan, and Eitan Tad-  
843 mor. Well-balanced schemes for the Euler equations with gravitation: Conservative  
844 formulation using global fluxes. *Journal of Computational Physics*, 2018.
- 845 [CK15] Praveen Chandrashekar and Christian Klingenberg. A second order well-balanced fi-  
846 nite volume scheme for Euler equations with gravity. *SIAM Journal on Scientific*  
847 *Computing*, 37(3):B382–B402, 2015.
- 848 [CL94] P Cargo and AY LeRoux. A well balanced scheme for a model of atmosphere with  
849 gravity. *COMPTEs RENDUS DE L ACADEMIE DES SCIENCES SERIE I-*  
850 *MATHEMATIQUE*, 318(1):73–76, 1994.
- 851 [DZBK14] Vivien Desveaux, Markus Zenk, Christophe Berthon, and Christian Klingenberg. A  
852 well-balanced scheme for the Euler equation with a gravitational potential. In  
853 *Finite Volumes for Complex Applications VII-Methods and Theoretical Aspects*,  
854 pages 217–226. Springer, 2014.
- 855 [DZBK16] Vivien Desveaux, Markus Zenk, Christophe Berthon, and Christian Klingenberg. A  
856 well-balanced scheme to capture non-explicit steady states in the Euler equations  
857 with gravity. *International Journal for Numerical Methods in Fluids*, 81(2):104–  
858 127, 2016.
- 859 [ER13] Timothy A Eymann and Philip L Roe. Multidimensional active flux schemes. In *21st*  
860 *AIAA computational fluid dynamics conference*, 2013.
- 861 [Fan17] Duoming Fan. *On the acoustic component of active flux schemes for nonlinear hyper-*  
862 *bolic conservation laws*. PhD thesis, University of Michigan, Dissertation, 2017.
- 863 [FR15] Doreen Fan and Philip L Roe. Investigations of a new scheme for wave propagation. In  
864 *22nd AIAA Computational Fluid Dynamics Conference*, page 2449, 2015.
- 865 [GL96] Joshua M Greenberg and Alain-Yves LeRoux. A well-balanced scheme for the numerical  
866 processing of source terms in hyperbolic equations. *SIAM Journal on Numerical*  
867 *Analysis*, 33(1):1–16, 1996.
- 868 [HKS19] Christiane Helzel, David Kerkmann, and Leonardo Scandurra. A new ADER method  
869 inspired by the active flux method. *Journal of Scientific Computing*, 80(3):1463–  
870 1497, 2019.
- 871 [KM16] R Käppeli and S Mishra. A well-balanced finite volume scheme for the Euler equations  
872 with gravitation-the exact preservation of hydrostatic equilibrium with arbitrary  
873 entropy stratification. *Astronomy & Astrophysics*, 587:A94, 2016.
- 874 [LeV98] Randall J LeVeque. Balancing source terms and flux gradients in high-resolution Go-  
875 dunov methods: the quasi-steady wave-propagation algorithm. *Journal of compu-*  
876 *tational physics*, 146(1):346–365, 1998.
- 877 [LGB11] Randall J LeVeque, David L George, and Marsha J Berger. Tsunami modelling with  
878 adaptively refined finite volume methods. *Acta Numerica*, 20:211–289, 2011.
- 879 [NR16] Hiroaki Nishikawa and Philip L Roe. Third-order active-flux scheme for advection  
880 diffusion: hyperbolic diffusion, boundary condition, and Newton solver. *Computers*  
881 *& Fluids*, 125:71–81, 2016.
- 882 [VL77] Bram Van Leer. Towards the ultimate conservative difference scheme. IV. A new ap-  
883 proach to numerical convection. *Journal of computational physics*, 23(3):276–299,  
884 1977.